COFUND. A project supported by the European Union

ATLAS measurements of the 125 GeV Higgs boson: Recent highlights and the charm frontier

IPPP Seminar

13th December 2018

Andy Chisholm
(CERN and University of Birmingham)

The Brout-Englert-Higgs Mechanism

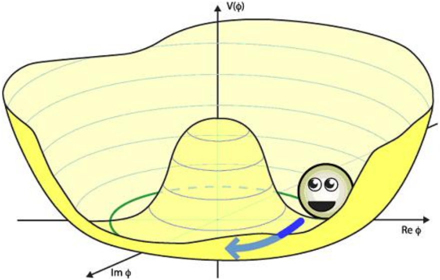

Figure from Philip Tanedo

- Introduce a complex scalar SU(2) doublet ϕ to the SM (4 d.o.f.)
- If potential $V(\phi)$ has a non-zero VEV, the EW symmetry is spontaneously broken
- Leads to Goldstone bosons (3 d.o.f.) which mix with $W^{\pm}$ and Z fields
- **Provides gauge invariant mass terms (and long. pol.) to the $W^{\pm}$ and Z ✓**
- **Predicts the fourth d.o.f. should manifest as a scalar "Higgs" boson!**

In 2012 a particle with a mass of 125 GeV, consistent with the SM Higgs boson, was discovered by ATLAS and CMS ✓

"Yukawa" couplings between the Higgs (ϕ) and fermion (ψ) fields are possible:

$$\mathcal{L}_{\text{fermion}} = -y_f \cdot \left[\bar{\psi}_L \phi \psi_R + \bar{\psi}_R \bar{\phi} \psi_L\right]$$

If $V(\phi)$ has a non-zero VEV, expansion leads to (h is the physical Higgs field):

$$\mathcal{L}_{\text{fermion}} = -\underbrace{\frac{y_f v}{\sqrt{2}} \cdot \bar{\psi}\psi}_{\text{mass term}} - \underbrace{\frac{y_f}{\sqrt{2}} \cdot h\bar{\psi}\psi}_{\text{Yukawa coupling term}}$$

Results in Higgs–fermion coupling proportional to the fermion mass ($g_{Hf\bar{f}} = m_f/v$)

- Gauge invariant fermion mass terms in SM ✓
- y_f "predicted" in SM given knowledge of v and m_f ($v \approx 246$ GeV from EW observables) ✓
- Offers no fundamental insight into the observed fermion mass hierarchy ✗

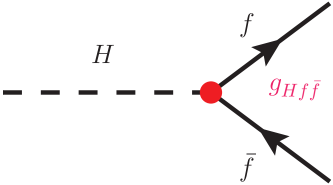

While Yukawa couplings provide concrete predictions for $Hf\bar{f}$ interactions, they fail to describe the origin of the fermion mass hierarchy i.e. why is $m_t/m_e \approx \mathcal{O}(10^5)$!?

Physics beyond the SM is clearly required to explain the fermion mass hierarchy!

General purpose detector, ideal tool (by design) to study the 125 GeV Higgs boson

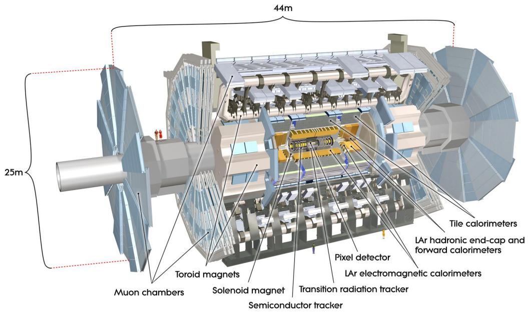

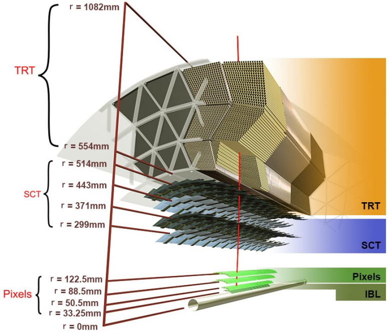

- **Inner Detector (ID):** Silicon Pixels and Strips (SCT) with Transition Radiation Tracker (TRT) $|\eta| < 2.5$ and (new for Run 2) Insertable B-Layer (IBL)
- **LAr EM Calorimeter:** Highly granular + longitudinally segmented (3-4 layers)
- **Had. Calorimeter:** Plastic scintillator tiles with iron absorber (LAr in fwd. region)
- **Muon Spectrometer (MS):** Triggering $|\eta| < 2.4$ and Precision Tracking $|\eta| < 2.7$
- **Jet Energy Resolution:** Typically $\sigma_E/E \approx 50\%/\sqrt{E(\text{GeV})} \oplus 3\%$
- **Track IP Resolution:** $\sigma_{d_0} \approx 60\,\mu\text{m}$ and $\sigma_{z_0} \approx 140\,\mu\text{m}$ for $p_T = 1$ GeV (with IBL)

ATLAS operated very successfully during the 2018 run! “Run 2” is now complete!

- Over 60 fb^{-1} of *pp* collisions recorded in 2018, most productive year of Run 2…
- **Final Run 2 $\sqrt{s} = 13$ TeV *pp* collision dataset of 149 fb^{-1} recorded!**
- Routinely “levelled” instantanous luminosity at 2×10^{34} cm^{-2}s^{-1}
- Operations and physics analysis in the presence of very high pileup now “routine”

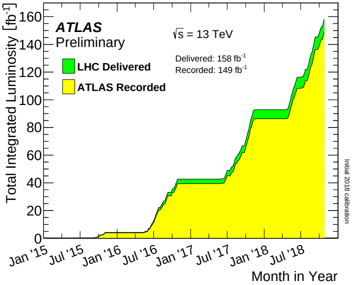

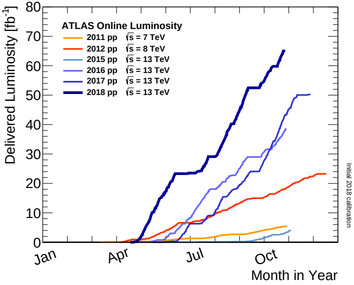

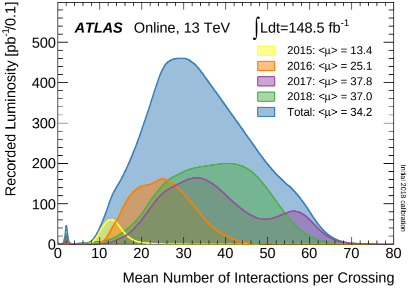

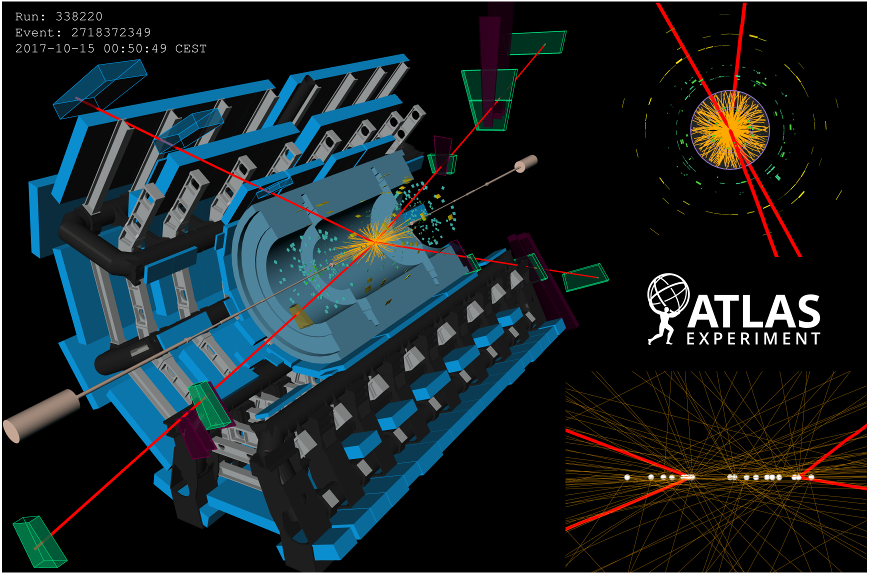

Two candidate $Z \rightarrow \mu^+\mu^-$ decays originating from independent *pp* interaction vertices associated with the same beam-crossing

Measurements of m_H (arXiv:1806.00242)

Latest combined measurement in $H \to 4\ell$ and $H \to \gamma\gamma$ channels, based on $36\,\text{fb}^{-1}$ of 13 TeV data and updated energy/momentum scale calibrations

- Per-event method used in $H \to 4\ell$ case, cross-checked with template method
- Likelihood fit with analytical PDF used for $H \to \gamma\gamma$ channel
- Uncertainty on combined m_H value dominated by systematics
- Precision improved from Summer 2017 result (ATLAS-CONF-2017-046), now on a par with Run 1 ATLAS + CMS

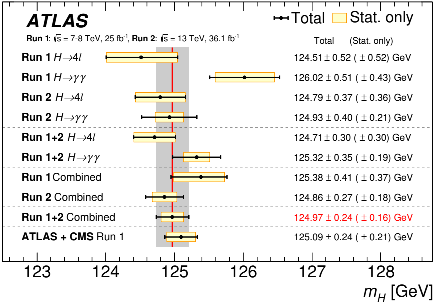

Run 2 $H \to \gamma\gamma$ systematics dominated

$$m_H = 124.97 \pm 0.24 \text{ GeV}$$

Source	Systematic uncertainty in m_H [MeV]
EM calorimeter response linearity	60
Non-ID material	55
EM calorimeter layer intercalibration	55
$Z \to ee$ calibration	45
ID material	45
Lateral shower shape	40
Muon momentum scale	20
Conversion reconstruction	20
$H \to \gamma\gamma$ background modelling	20
$H \to \gamma\gamma$ vertex reconstruction	15
e/γ energy resolution	15
All other systematic uncertainties	10

$H \to 4\ell$ still very statistically limited (bright prospects for potential Run 2 combination with CMS)

Ratio of on/off-shell signal strengths for $gg \to H \to VV^*$ sensitive to Γ_H

- Best direct limit from CMS $\Gamma_H < 1.10$ GeV at 95% CL with $H \to 4\ell$ (arXiv:1706.09936), very far from SM (≈ 4 MeV)
- Much more sensitive, though assmumes that any BSM physics would affect κ_g and κ_Z identically for on/off-shell production and not modify interference of S and B
- New result with $H \to ZZ^* \to 4\ell(\ell\ell\nu\nu)$ based on 80 fb^{-1} 13 TeV data

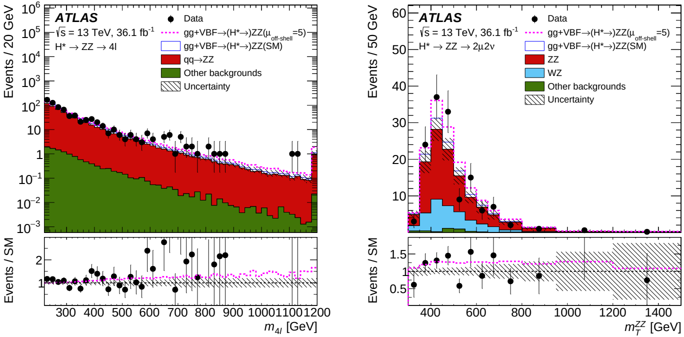

Observed (expected) upper limit of $\Gamma_H < 14.4(15.2)$ MeV at 95% CL

Measurements of Higgs boson production with bosonic channels

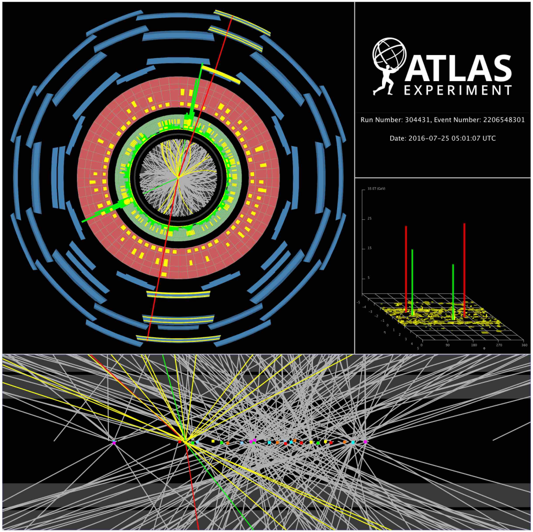

Candidate $H \to 2e2\mu$ event in 13 TeV data
with 25 additional reconstructed primary vertices

Measurements of Higgs boson production with bosonic channels

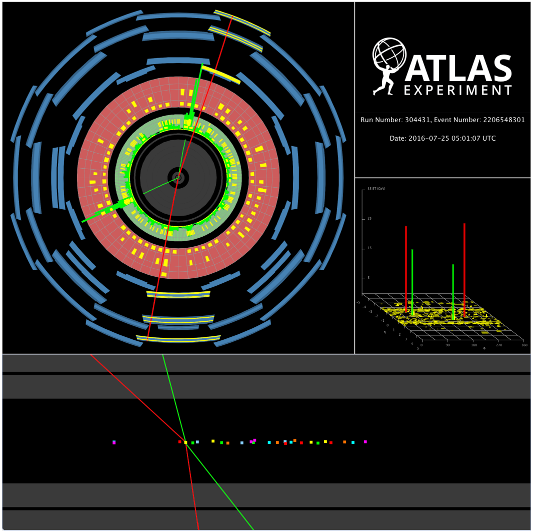

Candidate $H \to 2e2\mu$ event in 13 TeV data with 25 additional reconstructed primary vertices

$H \to \gamma\gamma$ production measurements recently updated with 80 fb^{-1} 13 TeV dataset

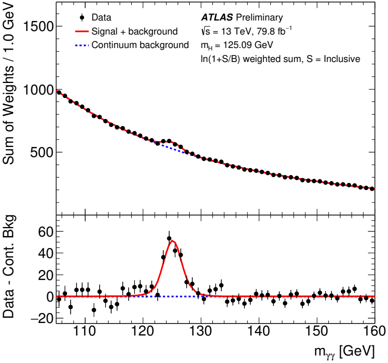

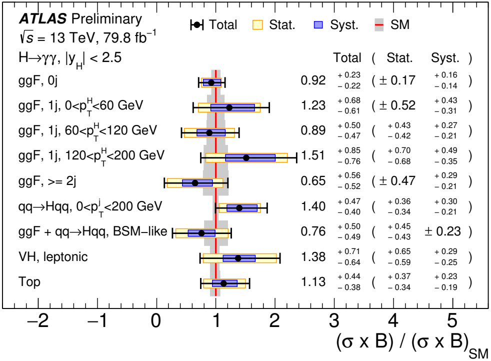

L: Inclusive $m_{\gamma\gamma}$ distribution (weighted) R: Summary of the measured simplified template cross sections (STXS)

- Wide range of inclusive and differential fiducial (phase space →) cross section measurements
- Global signal strength still consistent with SM
  $\mu = 1.06 \pm 0.08\,(\text{stat.})^{+0.08}_{-0.07}\,(\text{exp.})^{+0.07}_{-0.06}\,(\text{theo.})$

Objects	Definition
Photons	$\lvert\eta\rvert < 1.37$ or $1.52 < \lvert\eta\rvert < 2.37$, $p_T^{\text{iso},0.2}/p_T^{\gamma} < 0.05$
Jets	anti-k_t, $R = 0.4$, $p_T > 30\,\text{GeV}$, $\lvert y\rvert < 4.4$
– Central jets	$\lvert y\rvert < 2.5$
– b-jets	$\lvert y\rvert < 2.5$, $\Delta R(\text{jet}, b\text{-hadron}) < 0.4$ for b-hadrons with $p_T > 5$ GeV
Leptons, $\ell = e$ or μ	electrons: $p_T > 10\,\text{GeV}$, $\lvert\eta\rvert < 2.47$ (excluding $1.37 < \lvert\eta\rvert < 1.52$)
	muons: $p_T > 10\,\text{GeV}$, $\lvert\eta\rvert < 2.7$
Fiducial region	**Definition**
Diphoton fiducial	$N_\gamma \geq 2$, $p_T^{\gamma_1} > 0.35 \cdot m_{\gamma\gamma}$, $p_T^{\gamma_2} > 0.25 \cdot m_{\gamma\gamma}$
$N_{b\text{-jets}}$ measurement	Diphoton fiducial, $N_{\text{jets}}^{\text{Cen}} \geq 1$, $N_{\text{leptons}} = 0$

$H \to \gamma\gamma$ Differential Cross Sections: p_T^H (ATLAS-CONF-2018-028)

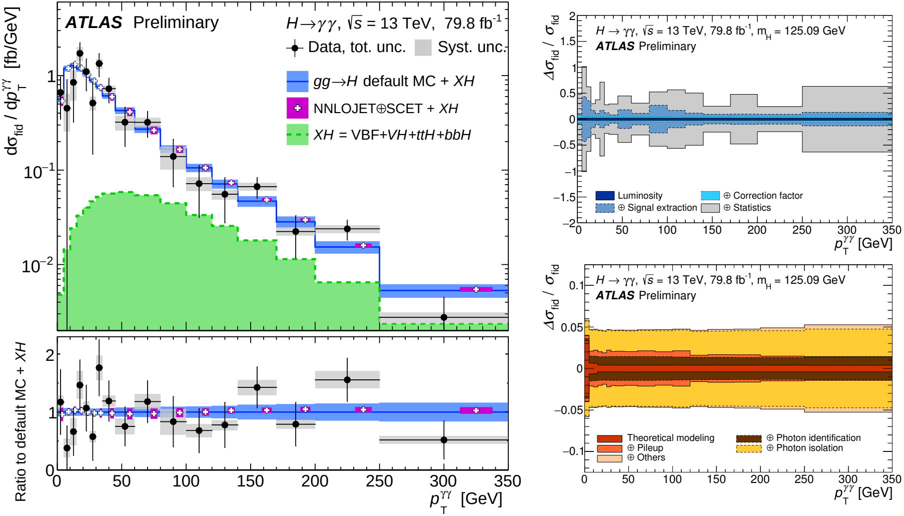

- χ^2 probability for compatiblity of data with default SM distribution† is 31%
- p_T^H exhibits lowest compatiblity with SM expected distribution (but still very high!)

† POWHEG NNLOPS normalised to YR4 N^{3}LO (QCD) and NLO(EW) cross section

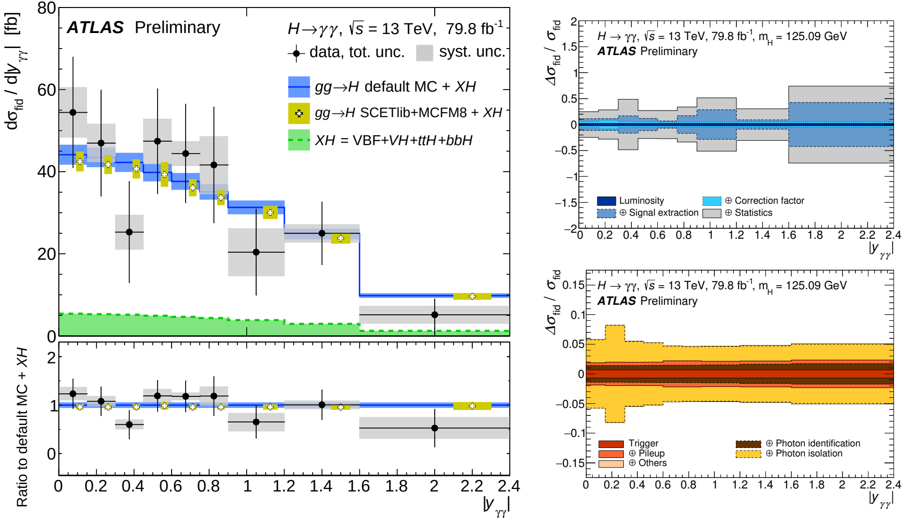

- χ^2 probability for compatiblity of data with default SM distribution† is 56%

† POWHEG NNLOPS normalised to YR4 N^3LO (QCD) and NLO(EW) cross section

$H \to \gamma\gamma$ Differential Cross Sections: p_T^{jet} (ATLAS-CONF-2018-028)

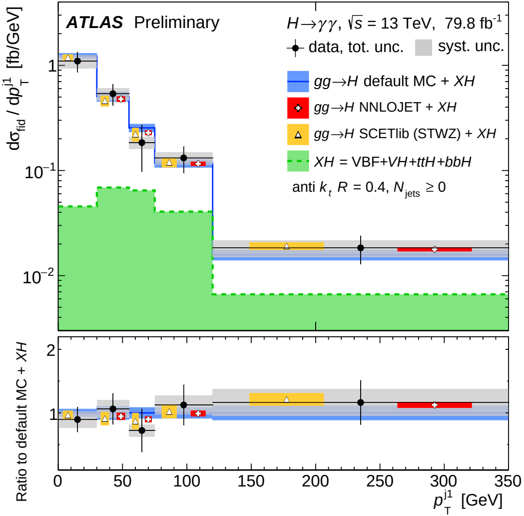

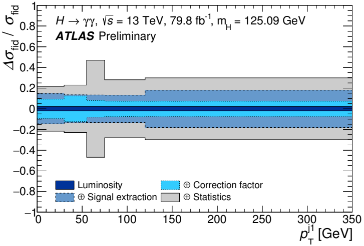

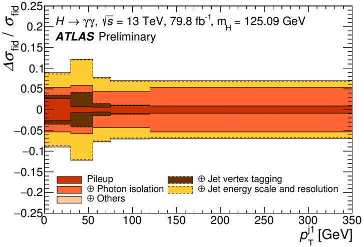

- Transverse momentum distribution of leading jet
- χ^2 probability for compatiblity of data with default SM distribution† is 88%

† POWHEG NNLOPS normalised to YR4 N^{3}LO (QCD) and NLO(EW) cross section

$H \rightarrow \gamma\gamma$ Differential Cross Sections: $N_{b\text{-jets}}$ (ATLAS-CONF-2018-028)

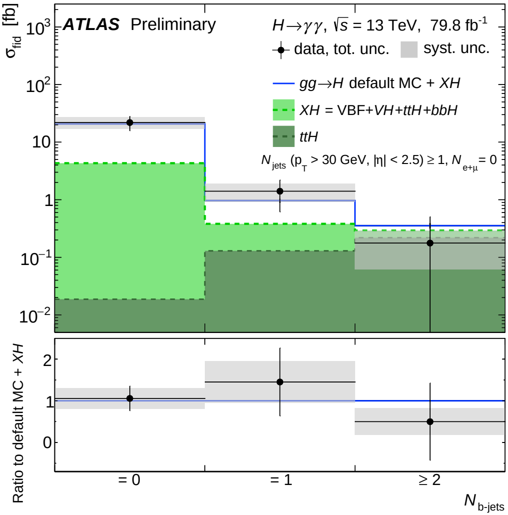

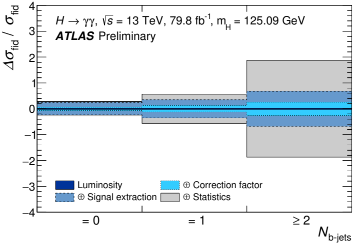

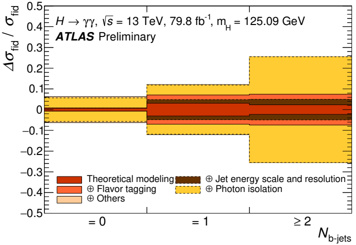

- Multiplicity of associated *b*-jets, sensitive to $t\bar{t}H$ and $b\bar{b}H$ production
- χ^2 probability for compatiblity of data with default SM distribution† is 84%

† POWHEG NNLOPS normalised to YR4 N^3LO (QCD) and NLO(EW) cross section

$H \to ZZ^* \to 4\ell$ production measurements updated with 80 fb^{-1} 13 TeV dataset, global signal strength $\mu = 1.19 \pm 0.19\,(\text{stat.}) \pm 0.06\,(\text{exp.})^{+0.08}_{-0.07}\,(\text{theo.})$

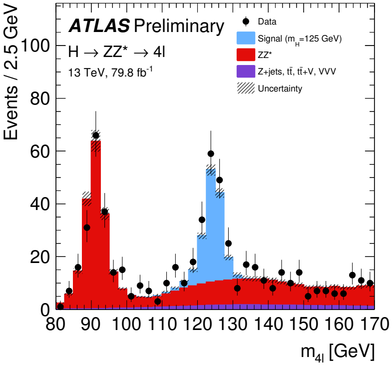

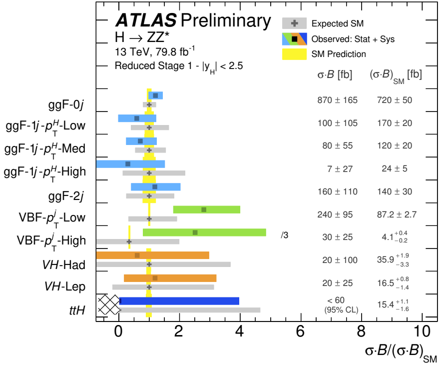

L: Inclusive $m_{4\ell}$ distribution R: "Reduced Stage 1" STXS

- Wide range of inclusive (fiducial and total) and fiducial differential cross section measurements
- Simple fiducial phase space →

Leptons and jets	
Leptons:	$p_T > 5$ GeV, $\vert\eta\vert < 2.7$
Jets:	$p_T > 30$ GeV, $\vert y\vert < 4.4$
remove jets with:	$\Delta R(\text{jet}, \ell) < 0.1$
Lepton selection and pairing	
Lepton kinematics:	$p_T > 20, 15, 10$ GeV
Leading pair (m_{12}):	SFOS lepton pair with smallest $\vert m_Z - m_{\ell\ell}\vert$
Subleading pair (m_{34}):	remaining SFOS lepton pair with smallest $\vert m_Z - m_{\ell\ell}\vert$
Event selection (at most one quadruplet per event)	
Mass requirements:	50 GeV$< m_{12} <$ 106 GeV and 12 GeV $< m_{34} <$ 115 GeV
Lepton separation:	$\Delta R(\ell_i, \ell_j) > 0.1$
J/ψ veto:	$m(\ell_i, \ell_j) > 5$ GeV for all SFOS lepton pairs
Mass window:	115 GeV $< m_{4\ell} <$ 130 GeV
If extra leptons with $p_T > 12$ GeV:	Quadruplet with the largest ME

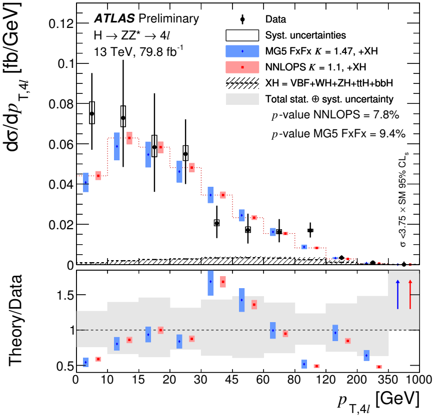

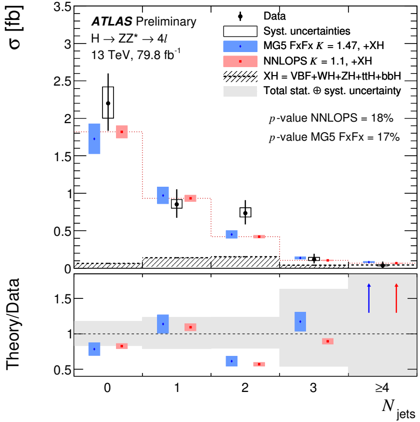

- Differential measurements of p_T^H and associated jet multiplicity
- p-values for compatiblity of data with predictions reasonably low...

Measurements of SM Higgs boson decays to bottom quarks

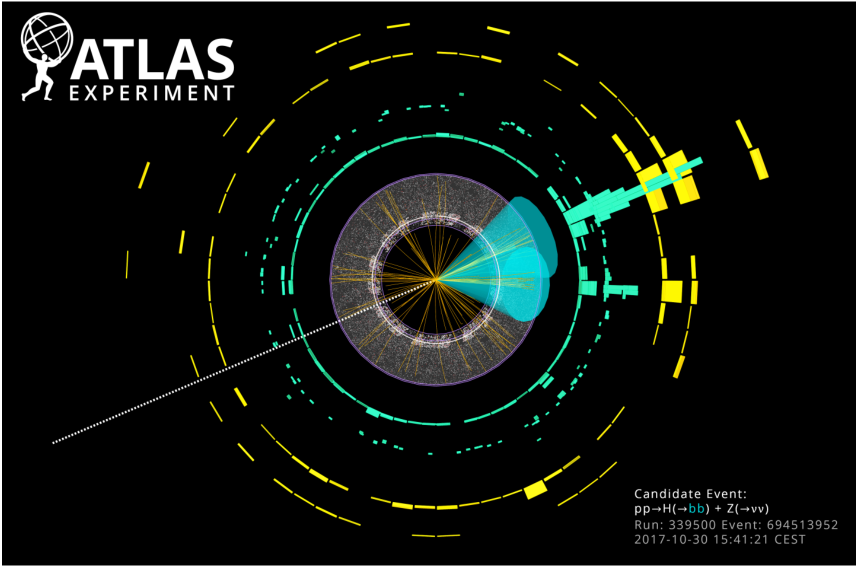

Candidate $pp \rightarrow Z(\nu\nu)H, H \rightarrow b\bar{b}$ event in 13 TeV data

VH channel traditionally expected to be brightest hope of finding $H \to b\bar{b}$ at LHC

- Search for events with 0, 1 or 2 leptons ($Z \to \nu\nu$, $W \to \ell\nu$ and $Z \to \ell\ell$) and ≥ 2 b-tagged jets, focus on high p_T^V events to suppress $V+$jets and $t\bar{t}$ background
- Recently **updated with 80 fb^{-1} of 13 TeV data** from LHC Run 2 (2015 - 2017)
- **BDT used as nominal S/B discriminant:** trained with kinematic variables (e.g. $m_{b\bar{b}}$, p_T^V, $E_{\mathrm{T}}^{\mathrm{miss}}$, ΔR_{bb}, p_{T}^{b} etc.) in each channel
- **Eight signal regions used:** (3 lepton multiplicity) $\times$ (2 jet multiplicity) $+$ 1 additional jet multiplicity and 1 additional p_T^V region for 2 lepton channel

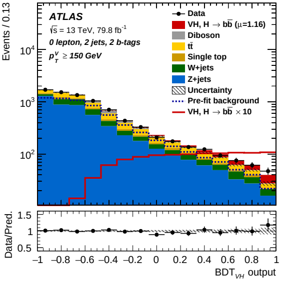

0 lepton (2 jets)

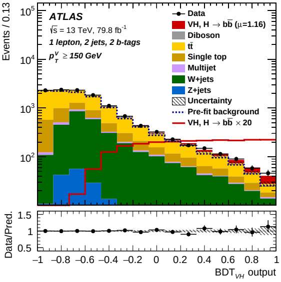

1 lepton (2 jets)

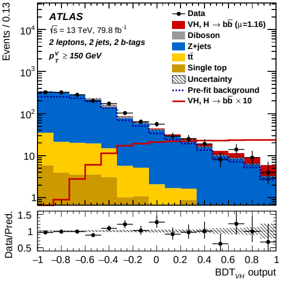

2 lepton (2 jets)

VH, $H \to b\bar{b}$ signal now very clearly visible by eye! For 13 TeV (Run 2) alone, observed (expected) significance is $4.9(4.3)\sigma$, signal strength $\mu_{VH(b\bar{b})} = 1.16^{+0.27}_{-0.25}$

- Cut-based analysis (CBA) also performed as a cross-check, selection performed using many of the same variables used in BDT
- Parallel "validation" analysis of $VZ(b\bar{b})$: $\mu = \mathbf{1.20 \pm 0.08\,(stat.)^{+0.19}_{-0.16}\,(syst.)}$

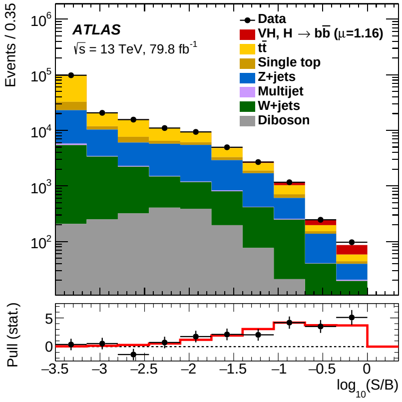

Combined $\log(S/B)$ distribution for multivariate analysis

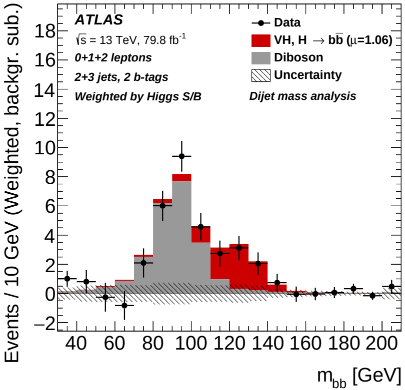

Bkgd. subtracted $m_{b\bar{b}}$ distribution for CBA, weighted by per-event S/B

Large reduction in systematic uncertainties achieved w.r.t. earlier 36 fb^{-1} Run 2 result (arXiv:1708.03299), though sensitivity still limited by systematics...

- "Theory" systematics remain largest for signal strength measurement, particularly signal and $V+$jets background modelling
- Experimental systematics dominated by b-tagging uncertainties

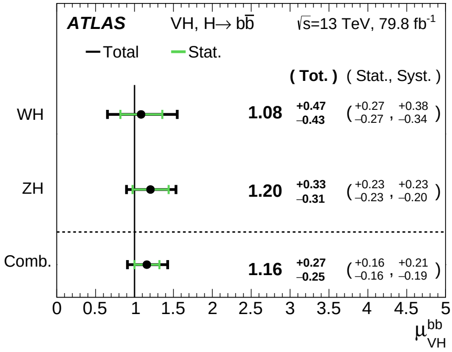

Source of uncertainty		σ_μ
Total		0.259
Statistical		0.161
Systematic		0.203
Experimental uncertainties		
Jets		0.035
E_T^{miss}		0.014
Leptons		0.009
b-tagging	b-jets	0.061
	c-jets	0.042
	light-flavour jets	0.009
	extrapolation	0.008
Pile-up		0.007
Luminosity		0.023
Theoretical and modelling uncertainties		
Signal		0.094
Floating normalisations		0.035
$Z+$ jets		0.055
$W+$ jets		0.060
$t\bar{t}$		0.050
Single top quark		0.028
Diboson		0.054
Multi-jet		0.005
MC statistical		0.070

Combination of all ATLAS searches for $H \to b\bar{b}$ decays performed, from both Run 2 (13 TeV) and Run 1 (7/8 TeV), three production channels considered:

- ***VH* production:** 80 fb^{-1} (13 TeV) + 20.3 fb^{-1} (8 TeV) + 4.7 fb^{-1} (7 TeV)
- **VBF + *ggH* production:** up to 30 fb^{-1} (13 TeV) + 20.2 fb^{-1} (8 TeV)
- **$t\bar{t}H$ production:** up to 36.1 fb^{-1} (13 TeV) + 20.3 fb^{-1} (8 TeV)

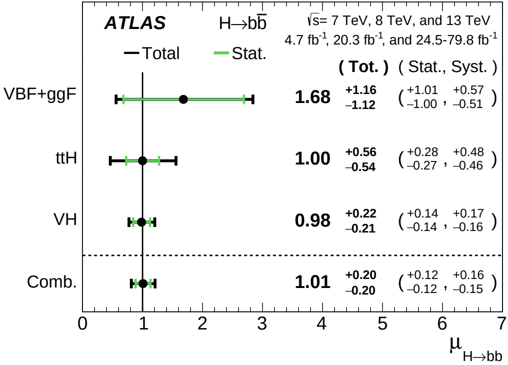

First observation of $H \to b\bar{b}$ decays!

Observed (expected) significance for $H \to b\bar{b}$ decay 5.4(5.5)σ (assuming relative production contributions from SM)

Channel	Significance	
	Exp.	Obs.
VBF+ggF	0.9	1.5
$t\bar{t}H$	1.9	1.9
VH	5.1	4.9
$H \to b\bar{b}$ combination	5.5	5.4

Combination of all ATLAS searches for *VH* production with 80 fb^{-1} of 13 TeV Run 2 data, three decays considered: $H \to b\bar{b}$, $H \to ZZ^*$ and $H \to \gamma\gamma$

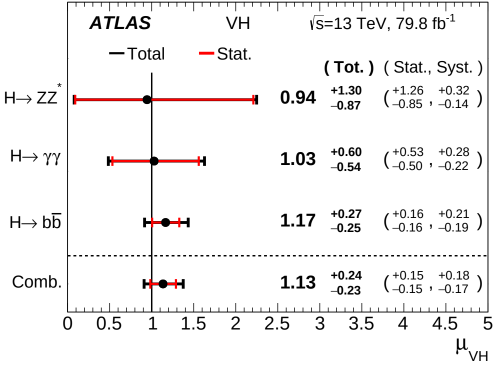

First observation of *VH* production with ATLAS data!

Observed (expected) significance for *VH* production 5.3(4.8)σ (assuming relative branching fractions from SM)

Channel	Significance Exp.	Significance Obs.
$H \to ZZ^* \to 4\ell$	1.1	1.1
$H \to \gamma\gamma$	1.9	1.9
$H \to b\bar{b}$	4.3	4.9
VH combined	4.8	5.3

Latest ATLAS 125 GeV Higgs combination with 13 TeV data

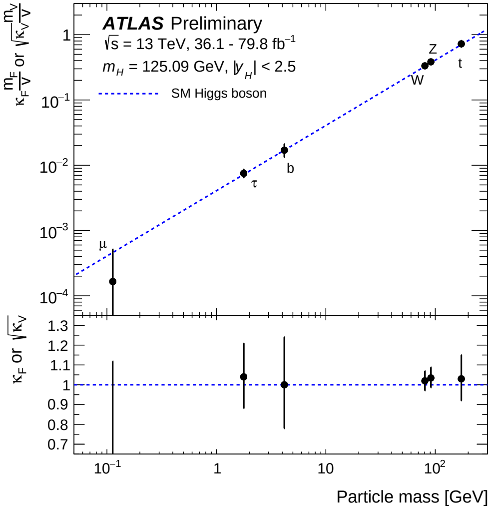

Reduced coupling strength modifiers as a function of fermion/boson mass, assuming no BSM contributions to Γ_H and the SM structure of loop processes

Latest combination of ATLAS measurements with all main channels probes compatiblity with SM production/decay properties

- Methodology similar (e.g. κ framework etc.) to well known Run 1 ATLAS+CMS combination (arXiv:1606.02266)
- All performed with 13 TeV data, several channels updated with 80 fb^{-1} dataset

Analysis	Integrated luminosity (fb^{-1})
$H \to \gamma\gamma$ (including $t\bar{t}H$, $H \to \gamma\gamma$)	79.8
$H \to ZZ^* \to 4\ell$ (including $t\bar{t}H$, $H \to ZZ^* \to 4\ell$)	79.8
$H \to WW^* \to e\nu\mu\nu$	36.1
$H \to \tau\tau$	36.1
VH, $H \to b\bar{b}$	36.1
$H \to \mu\mu$	79.8
$t\bar{t}H$, $H \to b\bar{b}$ and $t\bar{t}H$ multilepton	36.1

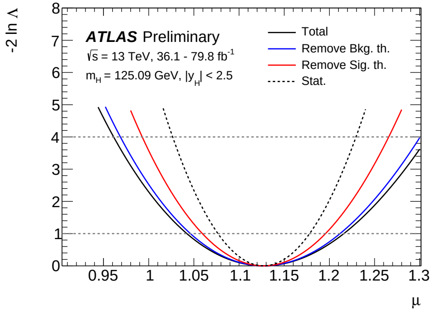

← **Global signal strength $\mu = 1.13^{+0.09}_{-0.08}$**

- Combined measurements lead to observed (expected) significance for VBF production of 6.5(5.3)σ
- VBF now observed by ATLAS experiment alone (following observation with ATLAS+CMS Run 1 combination)

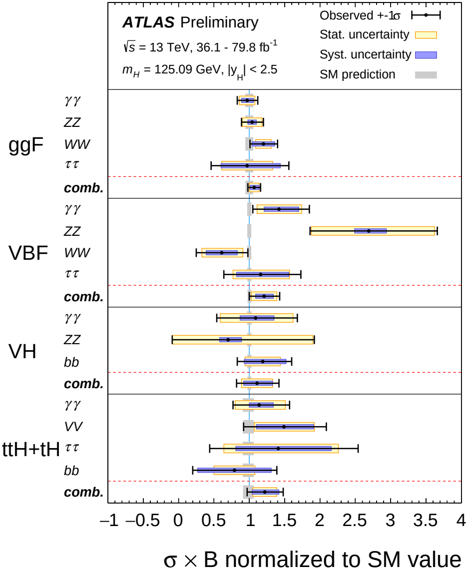

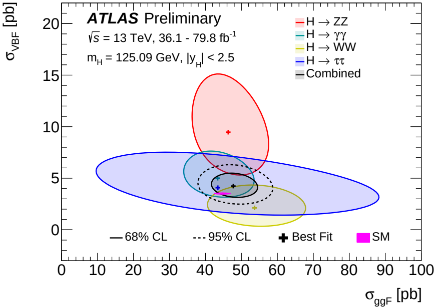

- Despite “hints” at $\geq 1\sigma$ deviations in global signal strengths for individual channels, combined measurements very compatible with SM

Branching fractions relative to SM prediction

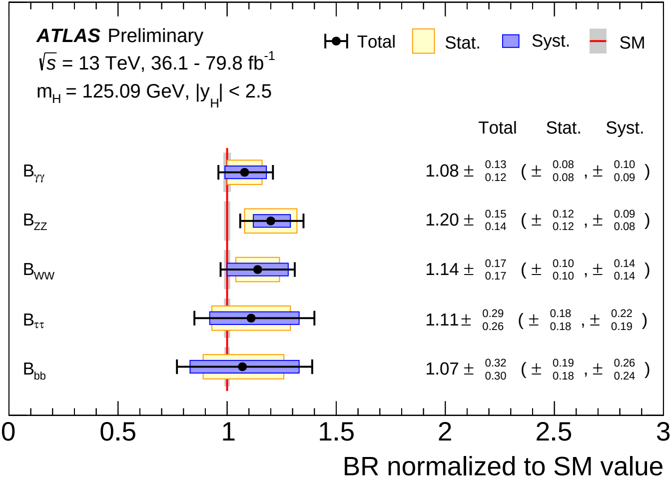

- Measured under the assumption of SM production

Ratios of inclusive cross-sections and branching fractions

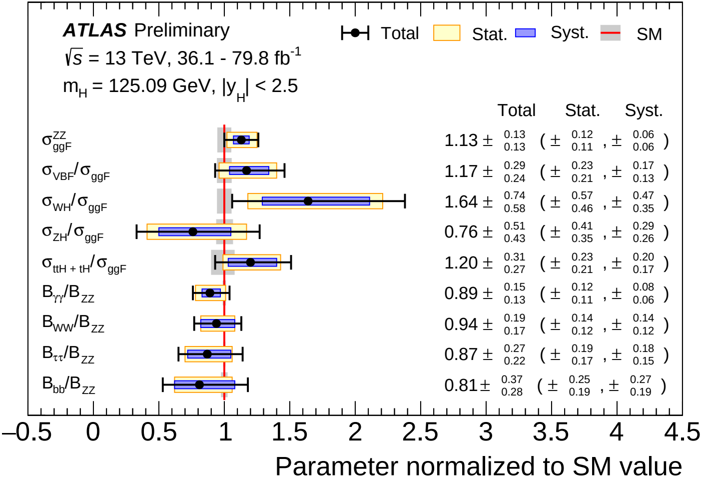

- $\sigma \times \mathcal{B}$ for $gg \to H \to ZZ^*$ used as reference

κ parameterisation including effective photon and gluon couplings

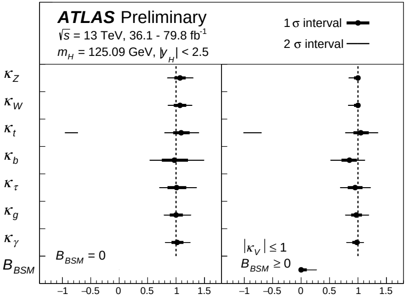

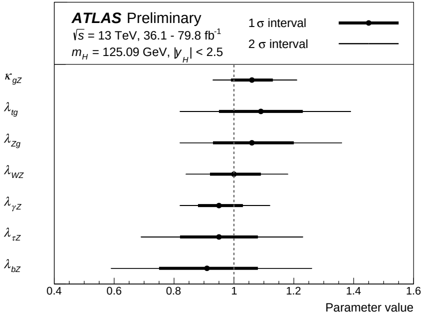

- Two possiblities for "BSM" contributions (BSM + invisible + inaccessible decays)
- **Left:** Assume no BSM contributions to the total width
- **Right:** Allow non-zero BSM contributions, but constrain $|\kappa_V| \leq 1$

- Consider ratios of coupling modifiers ($\lambda_{ij} = \kappa_i/\kappa_j$ and $\kappa gZ = \kappa_g \kappa_Z/\kappa_H$)
- Independent of model-dependent assumption on total width or BSM decays

Considering only κ_γ, κ_g, B_{BSM} as free parameters implies $B_{\text{BSM}} < 0.13$ at 95% CL

Executive Summary

- All main SM Higgs boson production processes (ggH, VBF, VH, $t\bar{t}H$) now firmly experimentally established ($\geq 5\sigma$)
- Observation of $H \to b\bar{b}$, $H \to \tau^+\tau^-$ and $H \to VV^{(*)}$ decays account for around 89% of the SM prediction for Γ_H
- Model independent measurements of ratios (where Γ_H cancels) of branching fractions and production cross-sections confirm SM-like relative couplings for W/Z bosons and the third generation fermions
- **No evidence for couplings to the first or second generation fermions**

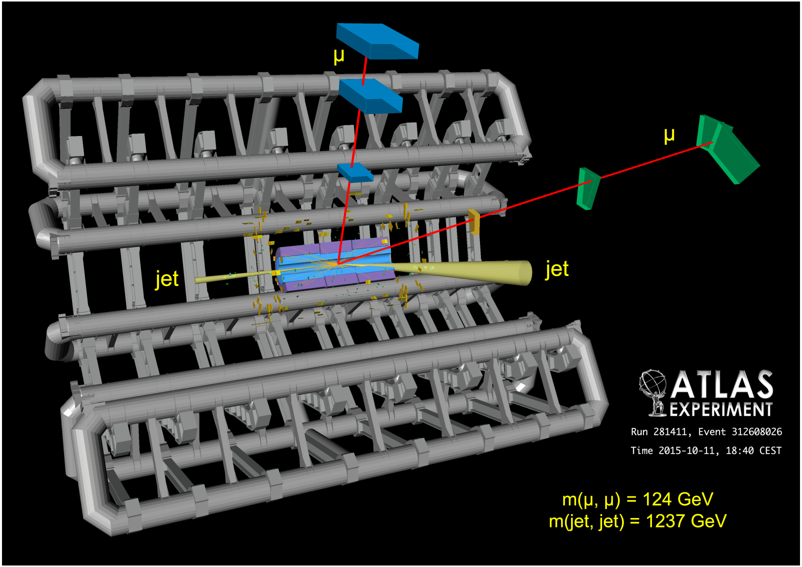

Candidate VBF $H \to \mu^+\mu^-$ event in 13 TeV data

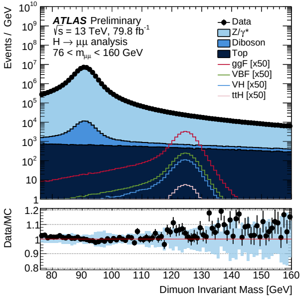

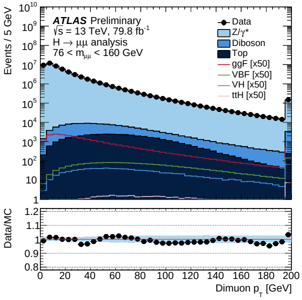

Most promising probe of SM Higgs coupling to second generation fermions

- Recently updated with 80 fb^{-1} of 13 TeV data
- Dominant backgound is $Z \to \mu^+\mu^-$(+jets), exploiting VBF production can help reduce this substantially
- Look for events with exactly two muons and classify them with BDT trained on variables sensitive to VBF production
- Define two VBF-like categories and split remaining ggH-like events into six categories based on $p_T^{\mu^+\mu^-}$ and $|\eta^\mu|$

	Z control region	$Z+\geq 2$ jets control region	VBF signal regions	ggF signal regions
Common	Primary vertex Two opposite-charge muons Muon: $\lvert\eta\rvert < 2.5$, $p_T^{\mathrm{lead}} > 27$ GeV, $p_T^{\mathrm{sublead}} > 15$ GeV No b-tagged jets $E_T^{\mathrm{miss}} < 80$ GeV			
Dimuon mass	$76 < m_{\mu\mu} < 106$ GeV		$110 < m_{\mu\mu} < 160$ GeV	
Jets	—	≥ 2 jets, each with $p_T > 25$ GeV and $\lvert\eta\rvert < 2.5$ or with $p_T > 30$ GeV and $2.5 < \lvert\eta\rvert < 4.5$		fail VBF selection

↑ **Definition of categories and control regions**

Search for $H \to \mu^+\mu^-$ II (ATLAS-CONF-2018-026)

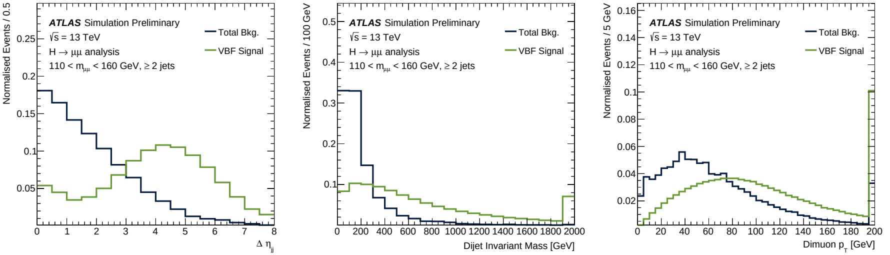

Boosted Decision Tree (BDT) for VBF events

- BDT trained on kinematic variables designed to separate VBF-like events from background
- Most sensitive variables (shown above) include m_{jj}, $\Delta\eta_{jj}$ and $p_T^{\mu^+\mu^-}$
- Two VBF categories ("Loose" and "Tight", white dashed lines) defined with BDT score →
- All remaining events enter the *ggH* category

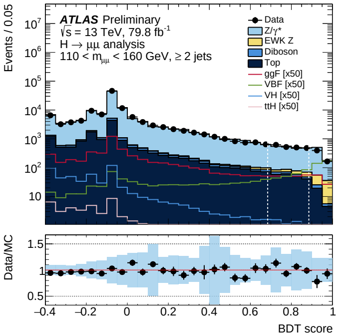

Search for $H \to \mu^+\mu^-$ III (ATLAS-CONF-2018-026)

$m_{\mu^+\mu^-}$ used as S/B discriminant, fit to each category using analytic functions for signal and background shape, fit result for most sensitive categories shown below

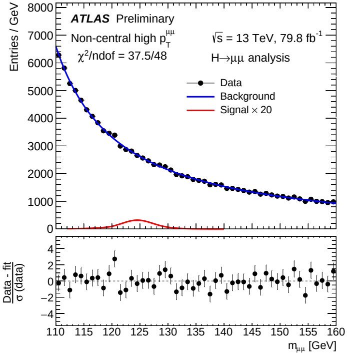

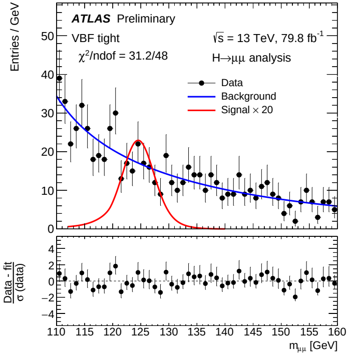

	Expected significance	Observed significance
Central low $p_T^{\mu\mu}$	0.10	−0.49
Non-central low $p_T^{\mu\mu}$	0.03	0.44
Central medium $p_T^{\mu\mu}$	0.31	1.55
Non-central medium $p_T^{\mu\mu}$	0.30	−1.16
Central high $p_T^{\mu\mu}$	0.38	0.48
Non-central high $p_T^{\mu\mu}$	0.43	0.15
VBF Loose	0.24	−0.88
VBF Tight	0.42	−0.26
Combined	0.88	0.04

Approaching sensitivity to SM prediction!

- Expected significance approaching 1σ, though downward fluctuation observed in data
- Measured signal strength $\mu = 0.1^{+1.0}_{-1.1}$
- Upper limit on $\sigma \times \mathcal{B}$ of 2.1×SM at 95% CL

$H \to \mathcal{M}\gamma$ decays provide a clean probe of the charm and light quark Yukawa couplings at the LHC

- $\mathcal{M}$ is a vector ($J^{PC} = 1^{--}$) light meson or quarkonium state such as $J/\psi, \psi(2S), \Upsilon(nS)$, $\phi(1020)$, $\rho(770)$
- **Interference** between **direct** ($H \to q\bar{q}$) and **indirect** ($H \to \gamma\gamma^*$) contributions
- **Direct** amplitude (upper) provides **sensitivity to the magnitude and sign of the $Hq\bar{q}$ couplings** (e.g. $\mathcal{M} = J/\psi$ sensitive to $Hc\bar{c}$ coupling)
- **Indirect** amplitude (lower) makes dominant contribution to decay width, **but not sensitive to Yukawa couplings**

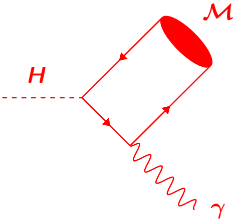

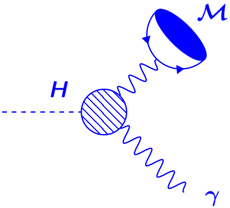

$$\mathcal{B}(H \to J/\psi\,\gamma) = (2.99 \pm 0.16) \times 10^{-6} \quad \dagger$$
$$\mathcal{B}(H \to \psi(2S)\,\gamma) = (1.03 \pm 0.06) \times 10^{-6} \quad \dagger$$
$$\mathcal{B}(H \to \phi\,\gamma) = (2.3 \pm 0.1) \times 10^{-6} \quad \ddagger$$
$$\mathcal{B}(H \to \rho\,\gamma) = (1.7 \pm 0.1) \times 10^{-5} \quad \ddagger$$

† Phys. Rev. D 90, 113010 (2014) (arXiv:1407.6695) ‡ JHEP 1508 (2015) 012 (arXiv:1505.03870)

Search for $H \to \phi/\rho\,\gamma$ Decays (arXiv:1712.02758)

Focus on dominant decays $\phi \to K^+K^-$ ($\mathcal{B} \approx 49\%$) and $\rho \to \pi^+\pi^-$ ($\mathcal{B} \approx 99\%$) and target high rate inclusive H production

Trigger and Data Sample

- Dedicated photon + di-track triggers implemented to identify distinctive event topology
- Collected up to **35.6 fb^{-1} $\sqrt{s}$ = 13 TeV *pp* dataset** during the 2015 and 2016 LHC runs

$\mathcal{M} = \{\phi, \rho\}$ Selection

- Require $m_{K^+K^-}$ or $m_{\pi^+\pi^-}$ consistent with ϕ or ρ meson mass
- **Minimum $p_T^{\mathcal{M}}$ requirement** varying with $m_{\mathcal{M}\gamma}$ from 40 – 47.2 GeV

Photon Selection

- "Tight" photon ID requirements
- Isolated in both tracker and calorimeter

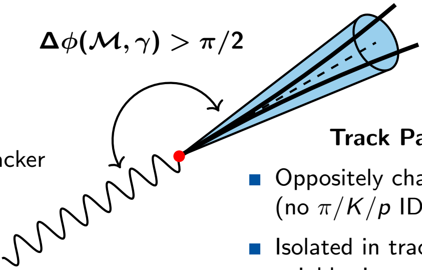

Track Pair Selection

- Oppositely charged pair of tracks (no $\pi/K/p$ ID applied)
- Isolated in tracker (accounting for neighboring track)

Search for $H \to \phi/\rho\gamma$ Decays - Results (arXiv:1712.02758)

- Invariant mass distributions of $K^+K^-\gamma$ (left) and $\pi^+\pi^-\gamma$ (right) candidates →
- Limit on $\mathcal{B}(H \to \phi\gamma)$ improved by almost 2× w.r.t. earlier ATLAS search
  (arXiv:1607.03400)

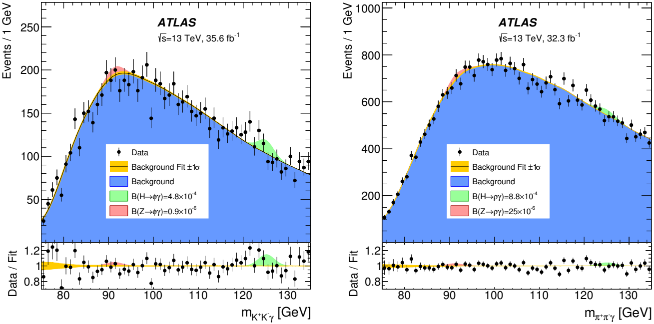

Observable	95% CL Upper Limit	
	Expected	Observed
$\mathcal{B}(H \to \phi\gamma)$	$(4.2^{+1.8}_{-1.2}) \times 10^{-4}$	4.8×10^{-4}
$\mathcal{B}(H \to \rho\gamma)$	$(8.4^{+4.1}_{-2.4}) \times 10^{-4}$	8.8×10^{-4}

World's first constraint on light quark Yukawa couplings from searches for $H \to \rho\gamma$ decays! (limit only $52 \times \mathcal{B}_{SM}$)

Focus on the experimentally clean $\psi(nS) \to \mu^+\mu^-$ decays and target high rate inclusive H production

Trigger and Data Sample

- Dedicated photon + single muon triggers implemented to identify distinctive event topology
- Collected **36.1 fb^{-1}** **$\sqrt{s} = 13$ TeV pp dataset** during the 2015 and 2016 LHC runs

$\psi(nS)$ Selection

- Require $m_{\mu^+\mu^-}$ loosely consistent with $\psi(nS)$ masses
- **Minimum $p_T^{\mathcal{M}}$ requirement** varying with $m_{\mathcal{M}\gamma}$ from 34 – 54.4 GeV

$p_T^{\mu\text{ lead}} > 18$ GeV

$p_T^{\mu\text{ sub-lead}} > 3$ GeV

$\Delta\phi(\mathcal{M}, \gamma) > \pi/2$

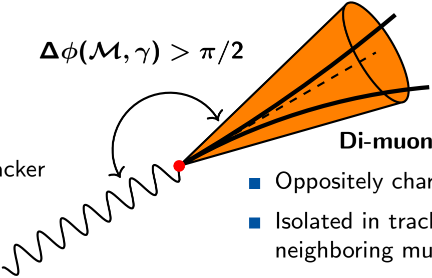

Photon Selection

- "Tight" photon ID requirements
- Isolated in both tracker and calorimeter

$p_T^{\gamma} > 35$ GeV

Di-muon Selection

- Oppositely charged pair of muons
- Isolated in tracker (accounting for neighboring muon track)
- $L_{xy}/\sigma_{L_{xy}} < 3$ to reject $b \to \psi(nS)$

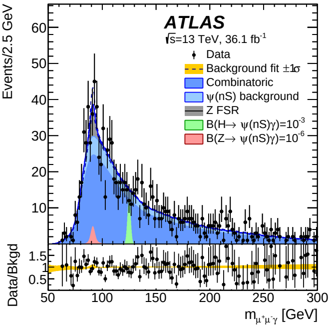

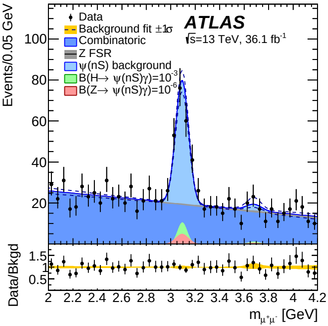

- Projections of fit ↑ to $\mu^+\mu^-\gamma$ (left) and $\mu^+\mu^-$ (right) invariant mass distributions

Observable	95% CL Upper Limit	
	Expected	Observed
$\mathcal{B}\,(H \rightarrow J/\psi\,\gamma)$	$(3.0^{+1.4}_{-0.8}) \times 10^{-4}$	3.5×10^{-4}
$\mathcal{B}\,(H \rightarrow \psi(2S)\,\gamma)$	$(15.6^{+7.7}_{-4.4}) \times 10^{-4}$	19.8×10^{-4}

World's first limit on $H \rightarrow \psi(2S)\,\gamma$ decays!

Limit on $\mathcal{B}(H \rightarrow J/\psi\,\gamma)$ improved by factor $\approx 4\times$ w.r.t. Run 1 result!

Run 1 $H \to J/\psi\,\gamma$ analysis projected to $\sqrt{s} = 14$ TeV scenario with 300(0) fb^{-1}

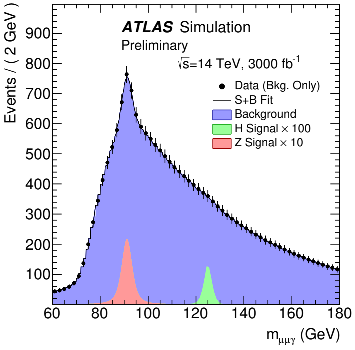

	Expected branching ratio limit at 95% CL		
	$\mathcal{B}(H \to J/\psi\gamma)$ [10^{-6}]		$\mathcal{B}(Z \to J/\psi\gamma)$ [10^{-7}]
	Cut Based	Multivariate Analysis	Cut Based
$300\,\text{fb}^{-1}$	185^{+81}_{-52}	153^{+69}_{-43}	$7.0^{+2.7}_{-2.0}$
$3000\,\text{fb}^{-1}$	55^{+24}_{-15}	44^{+19}_{-12}	$4.4^{+1.9}_{-1.1}$

	Standard Model expectation	
	$\mathcal{B}(H \to J/\psi\gamma)$ [10^{-6}]	$\mathcal{B}(Z \to J/\psi\gamma)$ [10^{-7}]
	2.9 ± 0.2	0.80 ± 0.05

- Optimistic scenario with MVA analysis still only sensitive to $\mathcal{B}(H \to J/\psi\,\gamma)$ at **15× SM value with 3000 fb^{-1}**

New ideas likely required to reach SM sensitivity in a HL-LHC scenario with this channel!

Search for $H \to c\bar{c}$ with $pp \to ZH$ production

Given the success of the W/Z associated production channel in observing $H \to b\bar{b}$ decays†, this channel is an obvious first candidate for a $H \to c\bar{c}$ search

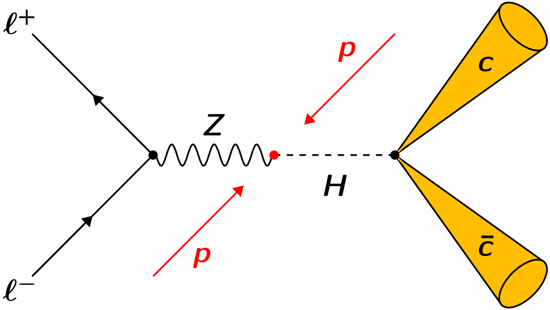

- **Focus on ZH production** with $Z \to e^+e^-$ and $Z \to \mu^+\mu^-$ decays for first ATLAS analysis: **Phys. Rev. Lett. 120 (2018) 211802, arXiv:1802.04329**
- Low exposure to experimental uncertainties, main backgrounds from $Z+$jets, $Z(W/Z)$ and $t\bar{t}$
- Pioneer use of **new c-tagging algorithm** developed by ATLAS for Run 2 to identify the experimental signature of an inclusive $H \to c\bar{c}$ decay

† ATLAS: Phys. Lett. B 786 (2018) 59 CMS: Phys. Rev. Lett. 121 (2018) 121801

New inclusive *c*-jet tagging algorithm developed by ATLAS for Run 2!

- Multivariate discriminant(s) built from input variables from low-level *b*-tagging algorithms (e.g. track impact parameter likelihood, secondary vertex finder)
- Trained with the same input variables used by the standard ATLAS Run 2 *b*-tagging algorithm (see ATL-PHYS-PUB-2015-022 for details)
- Implemented as two BDT discriminants, one trained to separate *c*-jets from *b*-jets (*x*-axis), another to separate *c*-jets from light-jets (*y*-axis)

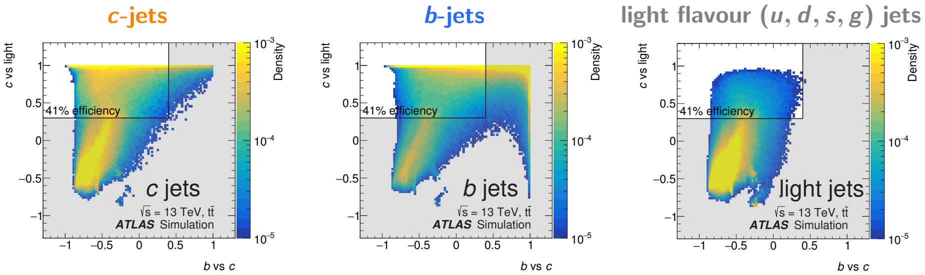

"*c*-tag" jets by making a cut in the 2D discriminant space, working point optimised for $H \to c\bar{c}$ limit is shown in the rectangular selection (shaded region rejected)

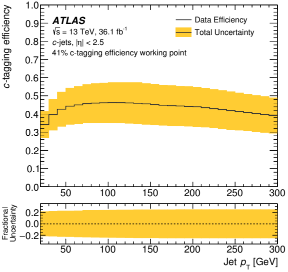

c-jets

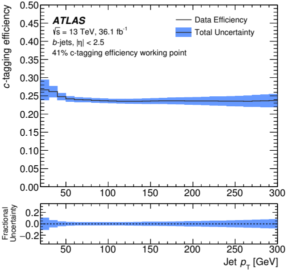

b-jets

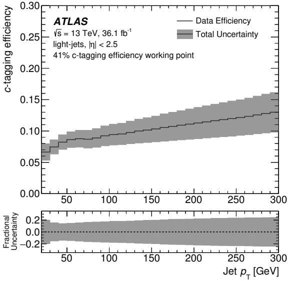

light flavour (u, d, s, g) jets

c-tagging efficiency for b-, c- and light flavour jets measured in data ↑

- Working point for $H \to c\bar{c}$ exhibits a c-jet tagging efficiency of around 40%
- Rejects b-jets by around a factor $4\times$ and light jets by around a factor $10\times$
- Efficiency calibrated in data with samples of b-jets from $t \to Wb$ decays and c-jets from $W \to cs, cd$ decays (in $t\bar{t}$ events)
- Typical total relative uncertainties of around **25%**, **5%** and **20%** for c-, b- and light jets, respectively

Use a $\sqrt{s} = 13$ TeV pp collision sample collected during 2015 and 2016 corresponding to an integrated luminosity of 36.1 fb^{-1}

$Z \to \ell^+\ell^-$ Selection

- Trigger with lowest available p_{T} single electron or muon triggers
- Exactly two same flavour reconstructed leptons (e or μ)
- Both leptons $p_{\mathrm{T}} > 7$ GeV and at least one with $p_{\mathrm{T}} > 27$ GeV
- Require opposite charges (dimuons only)
- $81 < m_{\ell\ell} < 101$ GeV
- $p_{\mathrm{T}}^{Z} > 75$ GeV

$H \to c\bar{c}$ Selection

- Consider anti-k_{T} $R = 0.4$ calorimeter jets with $|\eta| < 2.5$ and $p_{\mathrm{T}} > 20$ GeV
- At least two jets with leading jet $p_{\mathrm{T}} > 45$ GeV
- Form $H \to c\bar{c}$ candidate from the two highest p_{T} jets in an event
- At least one c-tagged jet from $H \to c\bar{c}$ candidate
- Dijet angular separation ΔR_{jj} requirement which varies with p_{T}^{Z}

Split events into 4 categories (with varying S/B) based on $H \to c\bar{c}$ candidates with 1 or 2 c-tags and p_{T}^{Z} above/below 150 GeV

Background Modelling

- Background dominated by $Z + \text{jets} \rightarrow$ (enriched in heavy flavour jets)
- Smaller contributions from $ZZ(q\bar{q})$, $ZW(q\bar{q}')$ and $t\bar{t}$
- Negligible ($< 0.5\%$) contributions from $W + \text{jets}$, WW, single-top and multi-jet

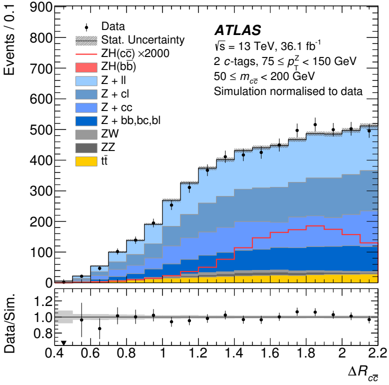

Simulation of $ZH(c\bar{c}/b\bar{b})$

- Normalised with LHC Higgs XS WG YR4 recommendations (arXiv:1610.07922)
- $ZH(b\bar{b})$ treated as background normalised to SM expectation (with th. uncertainty)

Process	MC Generator	Normalisation Cross section
$q\bar{q} \rightarrow ZH(c\bar{c}/b\bar{b})$	Powheg+GoSaM+MiNLO+Pythia8	NNLO (QCD) NLO (EW)
$gg \rightarrow ZH(c\bar{c}/b\bar{b})$	Powheg+Pythia8	NLO+NLL (QCD)
$Z + \text{jets}$	Sherpa 2.2.1	NNLO
ZZ and ZW	Sherpa 2.2.1	NLO
$t\bar{t}$	Powheg+Pythia8	NNLO+NNLL

The nominal MC generators used to model the signal and backgrounds

Background composition after *c*-tagging

↓ Left: 1 *c*-tag events

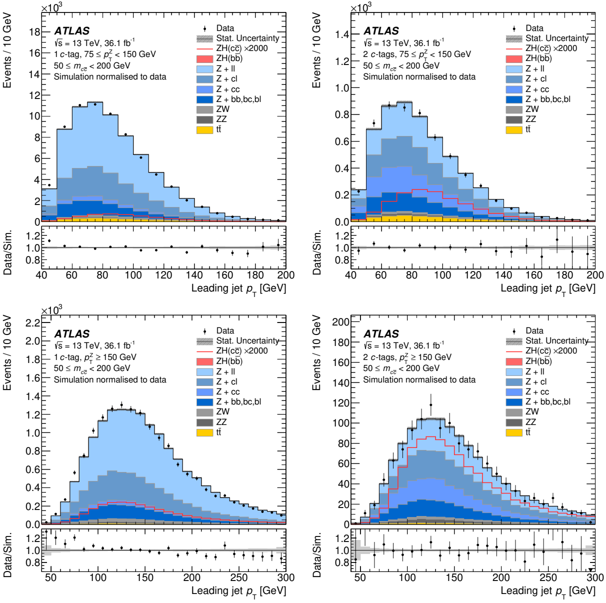

↑ Right: 2 *c*-tag events

Flavour composition of the $Z+$ jets sample enriched with c-jets

↓ Left: 1 c-tag events

↑ Right: 2 c-tag events

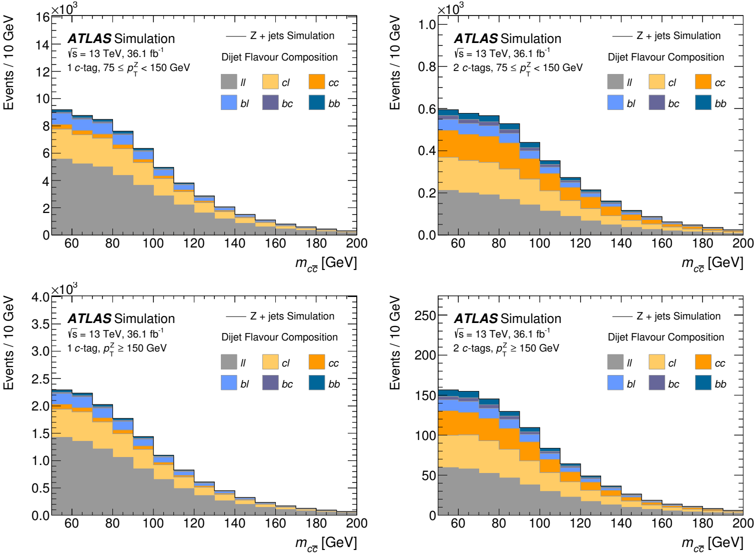

ZZ and ZW flavour composition after c-tagging

c-tagged ZZ and ZW production enriched in $Z \to c\bar{c}$ and $W \to cs, cd$ decays

↓ Left: 1 c-tag events

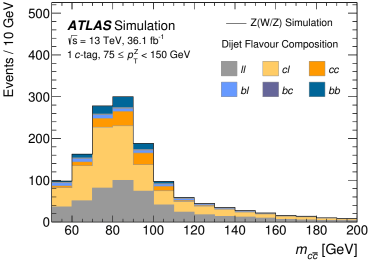

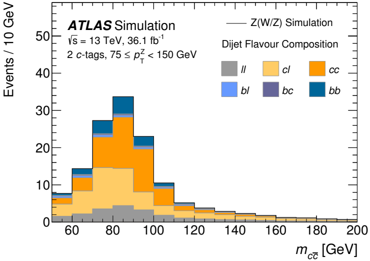

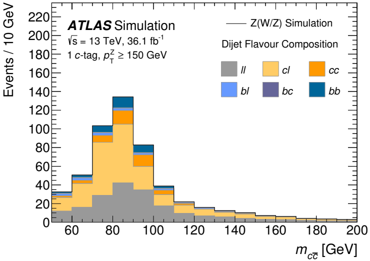

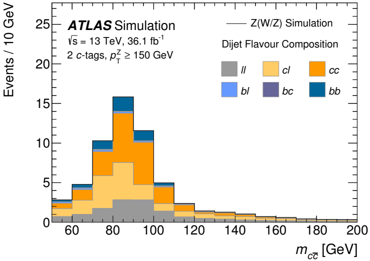

↑ Right: 2 c-tag events

Statistical Model

- Use the $H \to c\bar{c}$ candidate invariant mass $m_{c\bar{c}}$ as S/B discriminant
- Perform simultaneous binned likelihood fit to 4 categories within region $50 < m_{c\bar{c}} < 200$ GeV
- $ZH(c\bar{c})$ signal parameterised with free signal strength parameter, μ, common to all categories
- $Z +$ jets background determined directly from data with separate free normalisation parameter for each of the four categories

Systematic Uncertainties

- Included in the fit model as constrained nuisance parameters which parametrize the constraints from auxiliary measurements (e.g. lepton/jet calibrations)
- Experimental uncertainties associated with luminosity, c-tagging, lepton and jet performance are all included in the model
- Normalisation, acceptance and $m_{c\bar{c}}$ shape uncertainties associated with signal and background simulation are also included

Sensitivity dominated by systematic uncertainties, clear that these uncertainties should be reduced in order to fully exploit a larger dataset in the future

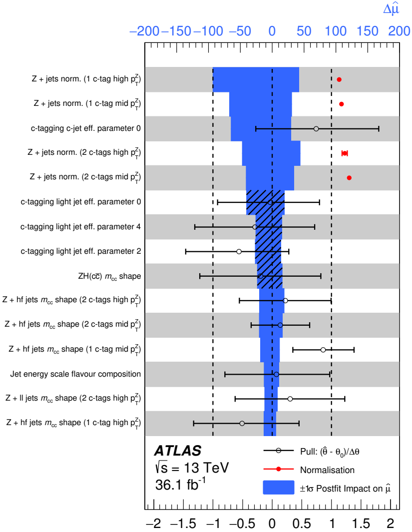

Source	$\sigma/\sigma_{\text{tot}}$
Statistical	49%
Floating $Z +$ jets Normalisation	31%
Systematic	87%
Flavour Tagging	73%
Background Modeling	47%
Lepton, Jet and Luminosity	28%
Signal Modeling	28%
MC statistical	6%

Note: correlations between nuisance parameters within groups leads to $\sum_i \sigma_i^2 \neq \sigma^2_{\text{syst.}}$

- c-tagging uncertainties and background modelling (particularly $Z +$ jets $m_{c\bar{c}}$ shape) have the dominant impact
- However, we can expect many of these uncertainties (e.g. $Z +$ jets norm.) to reduce with a larger dataset

1 c-tag | **2 c-tags**

$p_T^Z > 150$ GeV

$75 < p_T^Z < 150$ GeV

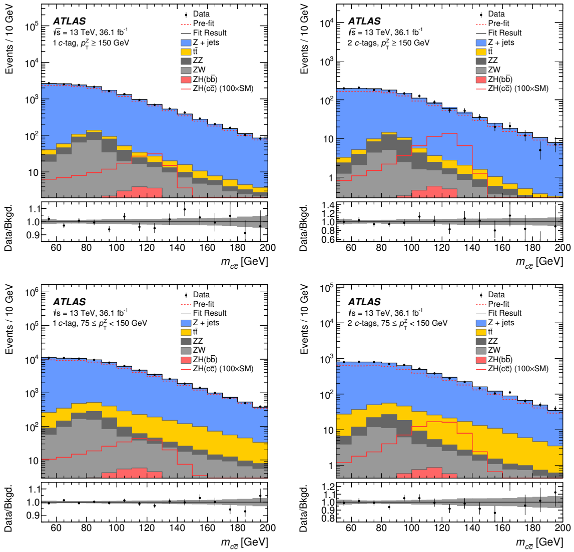

- No significant evidence for $ZH(c\bar{c})$ production
- Data consistent with background only hypothesis

SM expected number of $ZH(c\bar{c})$ events
1 c-tag $75 < p_T^Z < 150$ GeV
2.1
1 c-tag $p_T^Z > 150$ GeV
1.2
2 c-tags $75 < p_T^Z < 150$ GeV
0.5
2 c-tags $p_T^Z > 150$ GeV
0.3

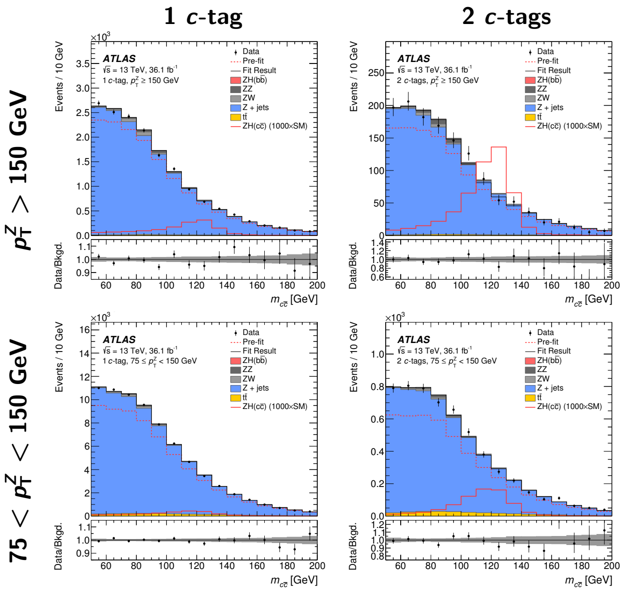

- No significant evidence for $ZH(c\bar{c})$ production
- Data consistent with background only hypothesis

SM expected number of $ZH(c\bar{c})$ events
1 c-tag $75 < p_T^Z < 150$ GeV
2.1
1 c-tag $p_T^Z > 150$ GeV
1.2
2 c-tags $75 < p_T^Z < 150$ GeV
0.5
2 c-tags $p_T^Z > 150$ GeV
0.3

Cross check with ZV production

- To validate background modelling and uncertainty prescriptions, measure production rate of the sum of ZZ and ZW relative to the SM expectation
- Observe (expect) ZV production with significance of 1.4σ (2.2σ)
- Measure ZV signal strength of $0.6^{+0.5}_{-0.4}$, consistent with SM expectation

Limits on $ZH(c\bar{c})$ production

95% CL CL_s upper limit on $\sigma(pp \to ZH) \times \mathcal{B}(H \to c\bar{c})$ [pb]			
Observed	Median Expected	Expected $+1\sigma$	Expected -1σ
2.7	3.9	6.0	2.8

- No evidence for $ZH(c\bar{c})$ production with current dataset (as expected)
- Upper limit of $\boldsymbol{\sigma(pp \to ZH) \times \mathcal{B}(H \to c\bar{c}) < 2.7}$ **pb** set at 95% CL, to be compared to an SM value of 2.55×10^{-2} pb
- Corresponds to **110**$\times$ (150^{+80}_{-40} expected) the SM expectation

World's most stringent direct constraint on $H \to c\bar{c}$ decays!

Interpreting the limit in terms of coupling constraints

⚠ **None of the following interpretation is sanctioned by ATLAS, responsibility lies solely with me!** However, everything is calculated using *published information alone*...

Ultimate goal is derive a model independent constraint on $Hc\bar{c}$ coupling, best way to do this is to exploit synergy with $ZH, H \to b\bar{b}$ channel

- Consider the ratio of $\mu_{ZH(c\bar{c})}/\mu_{ZH(b\bar{b})}$ for the $Z \to \ell^+\ell^-$ channel
- Sensitive to ratio κ_c/κ_b and independent of model dependent assumption on Γ_H
- Assume production is identical between $ZH(c\bar{c})$ and $ZH(b\bar{b})$ (i.e. selection phase space, categories etc.), leading to perfect cancellation of production cross-sections

$$\mu_{ZH(c\bar{c})} = \frac{\Gamma_{H\to c\bar{c}}}{\Gamma^{\text{SM}}_{H\to c\bar{c}}} \cdot \frac{\Gamma^{\text{SM}}_H}{\Gamma_H} \cdot \frac{\sigma(pp\to ZH)}{\sigma^{\text{SM}}(pp\to ZH)} = \kappa_c^2 \cdot \frac{\Gamma^{\text{SM}}_H}{\Gamma_H} \cdot \frac{\sigma(pp\to ZH)}{\sigma^{\text{SM}}(pp\to ZH)}$$

$$\mu_{ZH(b\bar{b})} = \frac{\Gamma_{H\to b\bar{b}}}{\Gamma^{\text{SM}}_{H\to b\bar{b}}} \cdot \frac{\Gamma^{\text{SM}}_H}{\Gamma_H} \cdot \frac{\sigma(pp\to ZH)}{\sigma^{\text{SM}}(pp\to ZH)} = \kappa_b^2 \cdot \frac{\Gamma^{\text{SM}}_H}{\Gamma_H} \cdot \frac{\sigma(pp\to ZH)}{\sigma^{\text{SM}}(pp\to ZH)}$$

$$\frac{\mu_{ZH(c\bar{c})}}{\mu_{ZH(b\bar{b})}} = \left(\frac{\kappa_c}{\kappa_b}\right)^2$$

- For now, consider systematic uncertainties for $ZH(c\bar{c})$ and $ZH(b\bar{b})$ as uncorrelated

What is the current sensitivity to κ_c/κ_b?

- Consider existing $ZH(c\bar{c})$ result and "combine" with recent ATLAS 80 fb^{-1} $Z(\ell\ell)H(b\bar{b})$ measurement†
- Small differences in selection and categories, but production cancellation hypothesis likely not too bad
- Treatment of systematics as un-correlated should give a more conservative constraint on κ_c/κ_b

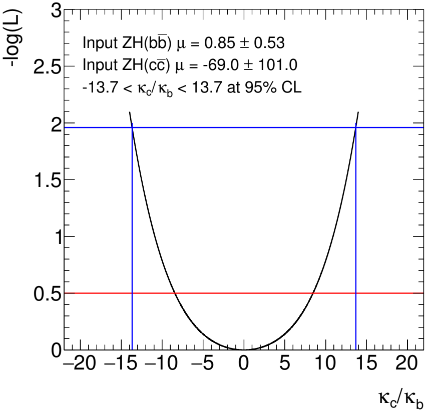

Existing results offer constraint at the level of $|\kappa_c/\kappa_b| < 14$ at 95% CL

- This is only possible when considering combination with $ZH(b\bar{b})$, not enough constraint (even with assumption for Γ_H) with $ZH(c\bar{c})$ analysis alone

† **Phys. Lett. B 786 (2018) 134 (arXiv:1807.00802)**

ATL-PHYS-PUB-2018-016

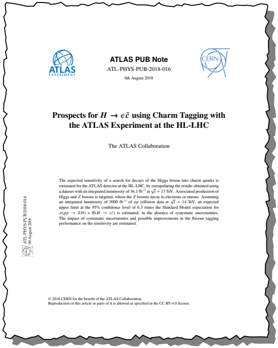

ATLAS PUB Note

ATL-PHYS-PUB-2018-016

8th August 2018

Prospects for $H \to c\bar{c}$ using Charm Tagging with the ATLAS Experiment at the HL-LHC

The ATLAS Collaboration

The expected sensitivity of a search for decays of the Higgs boson into charm quarks is estimated for the ATLAS detector at the HL-LHC, by extrapolating the results obtained using a dataset with an integrated luminosity of 36.1 fb^{-1} at $\sqrt{s}$ = 13 TeV. Associated production of Higgs and Z bosons is targeted, where the Z bosons decay to electrons or muons. Assuming an integrated luminosity of 3000 fb^{-1} of pp collision data at $\sqrt{s}$ = 14 TeV, an expected upper limit at the 95% confidence level of 6.3 times the Standard Model expectation for $\sigma(pp \to ZH) \times \mathcal{B}(H \to c\bar{c})$ is estimated, in the absence of systematic uncertainties. The impact of systematic uncertainties and possible improvements in the flavour tagging performance on the sensitivity are estimated.

ATL-PHYS-PUB-2018-016
08 August 2018

What sensitivity can we expect for a HL-LHC scenario with a $\sqrt{s} = 14$ TeV 3000 fb^{-1} dataset?

- A projection of the existing $Z(\ell\ell)H, H \to c\bar{c}$ analysis was prepared for the upcoming HL-LHC physics yellow report
- Generally very simiar to the Run 2 analysis, with several minor changes (described below)

Similarities

- Consider $Z(\ell\ell)H$ channel only (no addition of $W(\ell\nu)H$ or $Z(\nu\nu)H$)
- Identical event selection, categorisation and fit procedure

Differences

- Move to a tighter c-tagging working point (18% c-jet, 5% b-jets, 0.5% light jets)
- Don't consider systematic uncertainties (though their effect is estimated)

Prospects for $Z(\ell\ell)H, H \to c\bar{c}$ at the HL-LHC

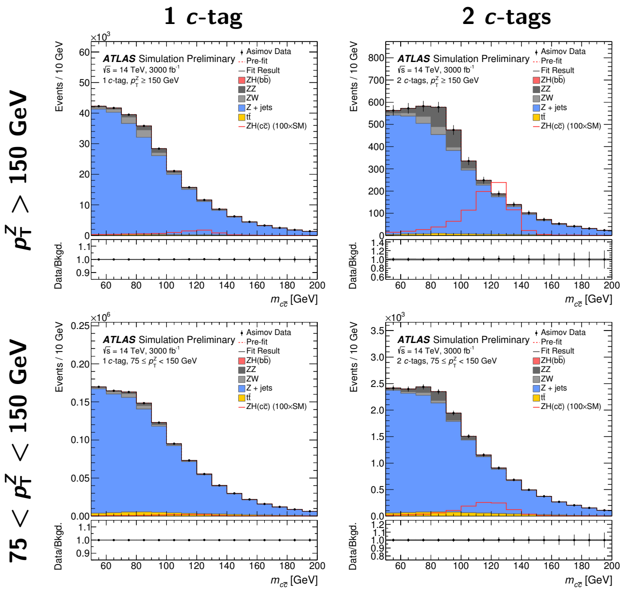

- Result of fit to expected ("Asimov") dataset for 3000 fb^{-1}
- Background composition (in terms of "process") very simiar
- Di-jet flavour composition now more c-jet enriched (you can't see that from these plots)

Projected Results

- Expected limit on $Z(\ell\ell)H, H \rightarrow c\bar{c}$ production at **6.3× SM prediction** at 95% CL (c.f. 150× expected for 36.1 fb^{-1} at 13 TeV)
- ⚠Corresponds to **around** $|\kappa_c/\kappa_b| < 3$ (with naive scaling of ATLAS Run 2 $ZH(b\bar{b})$ result based on luminosity only)

Things to remember

- Limit deteriorates by up to +36% with the inclusion of systematic uncertainties (estimated from Run 2 analysis)
- Projection considers the $\boldsymbol{Z(\ell\ell)H}$ **channel alone!** (sensitivity of $W(\ell\nu)H$ and $Z(\nu\nu)H$ channels at least as good)

⚠**As before, this is NOT an ATLAS result, but my estimate based on public information alone**

Status of ATLAS measurements of the 125 GeV Higgs boson in a nutshell

- All main SM production channels (ggH, VBF, VH and $t\bar{t}H$) firmly established experimentally, era of precision production measurements has begun
- Couplings of the Higgs boson to the W/Z bosons and third generation fermions established, behaviour very consistent with the SM expectation
- No evidence for Higgs boson couplings to the first and second generation fermions

ATLAS is pioneering a broad programme of searches for Higgs boson decays involving couplings to first and second generation fermions!

- Sensitivity to $H \to \mu^+\mu^-$ decays approaching the prediction for SM rate
- First constraints on $H \to \phi/\rho\,\gamma$ decays target light quark couplings
- Search for $ZH, H \to c\bar{c}$ production with c-tagging provides limit of 110× SM expectation, corresponds (roughly) to constraint of $|\kappa_c/\kappa_b| < 14$

Look out for further results with the full Run 2 dataset ($\approx$ 140 fb^{-1}) in the new year!

Thank you for your attention!

Additional Slides

Simplified Template Cross Sections (ATLAS-CONF-2018-028)

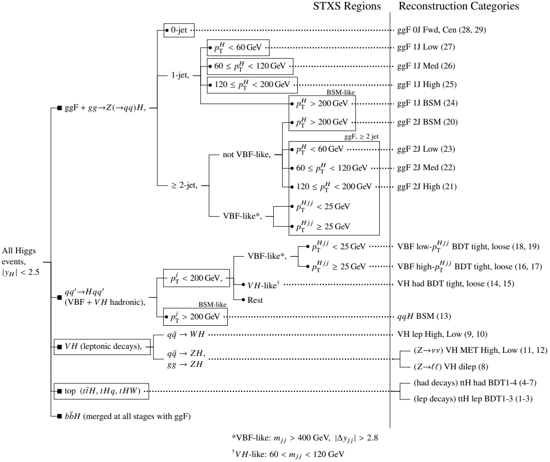

"STXS"

- Measurement strategy detailed in LHC-HXSWG YR4
- Cross section for Higgs production in for various sub-processes for a simplified fiducial volume of $|y_H| < 2.5$
- Theoretical uncertainties on signal cross sections removed (kept if they cause migration between categories)

Latest 13 TeV STXS measurements with $H \to \gamma\gamma$ using 80 fb^{-1}

- Mixed collection of nine "Stage 0" (■) and "Stage 1" regions (•) probed
- Some regions merged in this analysis (denoted by boxes) due to the limited sensitivity of dataset

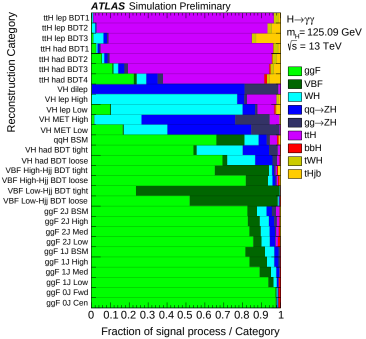
ATLAS Simulation Preliminary
H→γγ
m_H = 125.09 GeV
√s = 13 TeV
Reconstruction Category
ttH lep BDT1
ttH lep BDT2
ttH lep BDT3
ttH had BDT1
ttH had BDT2
ttH had BDT3
ttH had BDT4
VH dilep
VH lep High
VH lep Low
VH MET High
VH MET Low
qqH BSM
VH had BDT tight
VH had BDT loose
VBF High-Hjj BDT tight
VBF High-Hjj BDT loose
VBF Low-Hjj BDT tight
VBF Low-Hjj BDT loose
ggF 2J BSM
ggF 2J High
ggF 2J Med
ggF 2J Low
ggF 1J BSM
ggF 1J High
ggF 1J Med
ggF 1J Low
ggF 0J Fwd
ggF 0J Cen
ggF
VBF
WH
qq→ZH
gg→ZH
ttH
bbH
tWH
tHjb
0 0.1 0.2 0.3 0.4 0.5 0.6 0.7 0.8 0.9 1
Fraction of signal process / Category

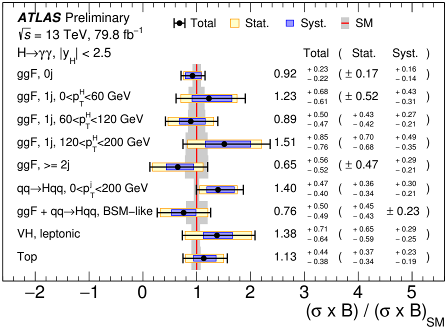
ATLAS Preliminary
√s = 13 TeV, 79.8 fb⁻¹
H→γγ, |y_H| < 2.5
Total Stat. Syst. SM
Total (Stat. Syst.)
ggF, 0j 0.92 +0.23 −0.22 (± 0.17 +0.16 −0.14)
ggF, 1j, 0<p_T^H<60 GeV 1.23 +0.68 −0.61 (± 0.52 +0.43 −0.31)
ggF, 1j, 60<p_T^H<120 GeV 0.89 +0.50 −0.47 (+0.43 −0.42 +0.27 −0.21)
ggF, 1j, 120<p_T^H<200 GeV 1.51 +0.85 −0.76 (+0.70 −0.68 +0.49 −0.35)
ggF, >= 2j 0.65 +0.56 −0.52 (± 0.47 +0.29 −0.21)
qq→Hqq, 0<p_T^j<200 GeV 1.40 +0.47 −0.40 (+0.36 −0.34 +0.30 −0.21)
ggF + qq→Hqq, BSM−like 0.76 +0.50 −0.49 (+0.45 −0.43 ± 0.23)
VH, leptonic 1.38 +0.71 −0.64 (+0.65 −0.59 +0.29 −0.25)
Top 1.13 +0.44 −0.38 (+0.37 −0.34 +0.23 −0.19)
−2 −1 0 1 2 3 4 5
(σ x B) / (σ x B)_SM

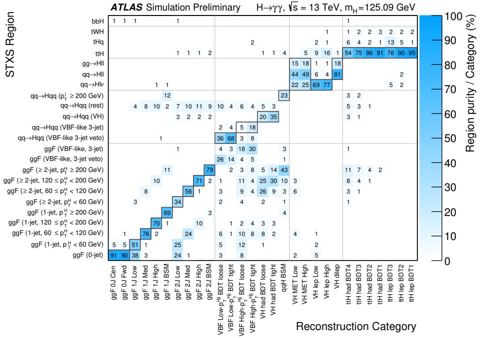
ATLAS Simulation Preliminary H→γγ, √s = 13 TeV, m_H=125.09 GeV
STXS Region
bbH
tWH
tHq
ttH
gg→Hll
qq→Hll
qq→Hlν
qq→Hqq (p_T^j ≥ 200 GeV)
qq→Hqq (rest)
qq→Hqq (VH)
qq→Hqq (VBF-like 3-jet)
qq→Hqq (VBF-like 3-jet veto)
ggF (VBF-like, 3-jet)
ggF (VBF-like, 3-jet veto)
ggF (≥ 2-jet, p_T^H ≥ 200 GeV)
ggF (≥ 2-jet, 120 ≤ p_T^H < 200 GeV)
ggF (≥ 2-jet, 60 ≤ p_T^H < 120 GeV)
ggF (≥ 2-jet, p_T^H < 60 GeV)
ggF (1-jet, p_T^H ≥ 200 GeV)
ggF (1-jet, 120 ≤ p_T^H < 200 GeV)
ggF (1-jet, 60 ≤ p_T^H < 120 GeV)
ggF (1-jet, p_T^H < 60 GeV)
ggF (0-jet)
ggF 0J Cen
ggF 0J Fwd
ggF 1J Low
ggF 1J Med
ggF 1J High
ggF 1J BSM
ggF 2J Low
ggF 2J Med
ggF 2J High
ggF 2J BSM
VBF Low-p_T^Hjj BDT loose
VBF Low-p_T^Hjj BDT tight
VBF High-p_T^Hjj BDT loose
VBF High-p_T^Hjj BDT tight
VH had BDT loose
VH had BDT tight
qqH BSM
VH MET Low
VH MET High
VH lep Low
VH lep High
VH dilep
ttH had BDT4
ttH had BDT3
ttH had BDT2
ttH had BDT1
ttH lep BDT3
ttH lep BDT2
ttH lep BDT1
Reconstruction Category
Region purity / Category (%)
0 10 20 30 40 50 60 70 80 90 100

Search for $H \rightarrow b\bar{b}$ decays in VBF($+\gamma$) events with 25 – 31 fb^{-1} of 13 TeV data

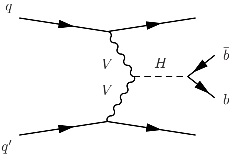

All-hadronic Channel

- Select two b-tagged jets along with "typical" VBF selection (two jets with a large $\Delta\eta$)
- BDT trained on kinematic variables used to define VBF rich categories, $m_{b\bar{b}}$ used as primary S/B discriminant

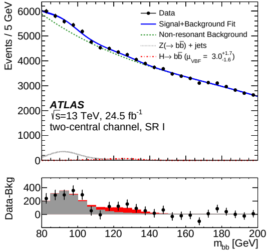

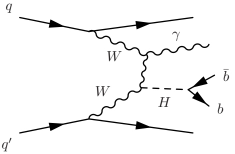

Photon Channel

- Similar to all-hadronic channel with additional requirement of a reconstructed isolated photon
- Photon effective in reducing dominant gluon-rich $bbjj$ background, enriching VBF purity

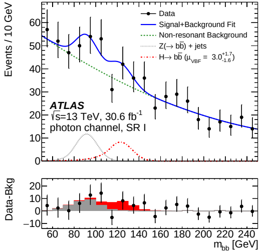

$m_{b\bar{b}}$ distributions for highest purity categories shown for both channels (right ↑)

$H \rightarrow b\bar{b}$ with VBF production II (arXiv:1807.08639)

Approaching SM sensitivity, combined observed (expected) 95% CL upper limit on overall signal strength (VBF had. + γ) of $5.9(3.0^{+1.3}_{-0.8})$

- Sensitivity dominated by statistical uncertainty
- Experimental uncertainties dominanted by understaning of jet performance

Uncertainty	$\sigma(\mu_H)$	$\sigma(\mu_{\text{VBF}})$
Total stat. uncertainty	$+1.3$ -1.3	$+1.6$ -1.5
Data stat. uncertainty	$+0.6$ -0.6	$+0.9$ -0.9
Non-resonant bkg	$+1.0$ -1.0	$+1.2$ -1.2
Z+jets normalization	$+0.5$ -0.5	$+0.5$ -0.5
Total syst. uncertainty	$+0.6$ -0.4	$+0.6$ -0.5
Higgs boson modeling	$+0.3$ -0.1	$+0.2$ -0.1
JES/JER	$+0.3$ -0.2	$+0.4$ -0.2
b-tagging (incl. trigger)	$+0.2$ -0.1	$+0.2$ -0.1
Other exp. uncertainty	$+0.4$ -0.3	$+0.4$ -0.4
Total	$+1.4$ -1.3	$+1.7$ -1.6

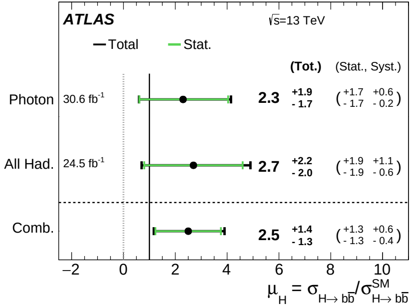

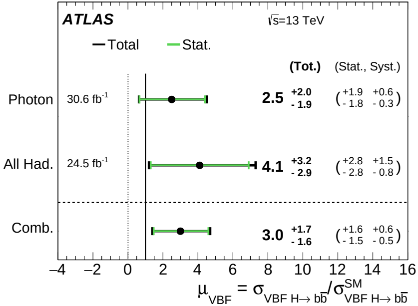

Measured signal strength for inclusive production (left) and VBF production (right) assuming SM contributions from *ggH*, *VH*, $t\bar{t}H$ production

Measurements of m_H (arXiv:1806.00242)

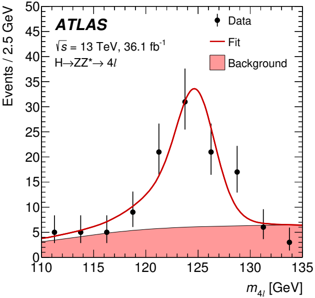

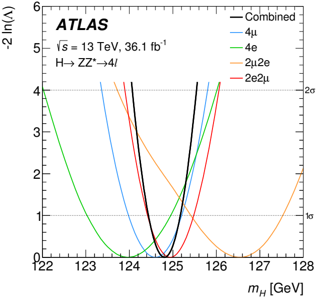

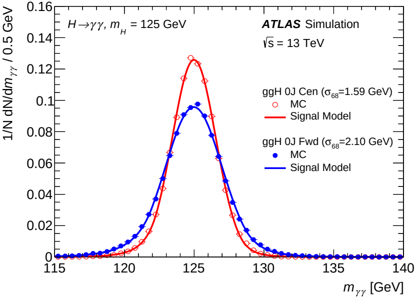

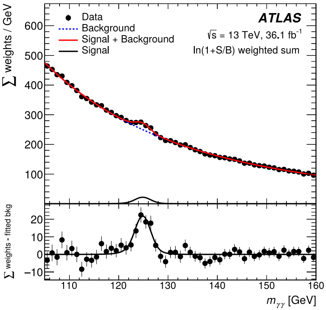

- Both signal $gg \rightarrow (H^*)ZZ^*$ and continuum background $gg \rightarrow ZZ$ simulated including interference with Sherpa 2.2.2 + OpenLoops
- Electroweak production of $pp \rightarrow VV + 2j$ (inc. VBF and VH) simulated with MadGraph5_aMC@ NLO
- Dominant background from $q\bar{q} \rightarrow ZZ$ simulated with Sherpa 2.2.2 (MEPS@NLO merging used, NLO EW corrections applied as function of m_{ZZ})

$$\mu_{\text{off-shell}} = \frac{\sigma^{gg\rightarrow H^*\rightarrow ZZ}_{\text{off-shell}}}{\sigma^{gg\rightarrow H^*\rightarrow ZZ}_{\text{off-shell,SM}}} = \kappa^2_{g,\text{off-shell}} \cdot \kappa^2_{Z,\text{off-shell}},$$

$$\mu_{\text{on-shell}} = \frac{\sigma^{gg\rightarrow H\rightarrow ZZ^*}_{\text{on-shell}}}{\sigma^{gg\rightarrow H\rightarrow ZZ^*}_{\text{on-shell,SM}}} = \frac{\kappa^2_{g,\text{on-shell}} \cdot \kappa^2_{Z,\text{on-shell}}}{\Gamma_H/\Gamma_H^{\text{SM}}},$$

$$\begin{aligned}
\sigma_{gg\rightarrow(H^*\rightarrow)ZZ}(\mu_{\text{off-shell}}) &= \mu_{\text{off-shell}} \cdot 1.2 \cdot K^{\text{S}}(m_{ZZ}) \cdot \sigma^{\text{SM}}_{gg\rightarrow H^*\rightarrow ZZ} \\
&+ \sqrt{\mu_{\text{off-shell}}} \cdot 1.2 \cdot K^{\text{I}}(m_{ZZ}) \cdot \sigma^{\text{SM}}_{gg\rightarrow ZZ,\,\text{Interference}} \\
&+ 1.2 \cdot K^{\text{B}}(m_{ZZ}) \cdot \sigma^{\text{SM}}_{gg\rightarrow ZZ,\,\text{cont}}\,, \\
\sigma^{\text{SM}}_{gg\rightarrow ZZ,\,\text{Interference}} &= \sigma^{\text{SM}}_{gg\rightarrow(H^*\rightarrow)ZZ} - \sigma^{\text{SM}}_{gg\rightarrow H^*\rightarrow ZZ} - \sigma^{\text{SM}}_{gg\rightarrow ZZ,\,\text{cont}}\,.
\end{aligned}$$

Process	Generator	Showering	PDF set	σ [pb] $\sqrt{s} = 13$ TeV	Order of σ calculation
ggF	POWHEG NNLOPS	PYTHIA 8	PDF4LHC15	48.52	$N^3LO(QCD)+NLO(EW)$
VBF	POWHEG-BOX	PYTHIA 8	PDF4LHC15	3.78	approximate-NNLO(QCD)+NLO(EW)
WH	POWHEG-BOX	PYTHIA 8	PDF4LHC15	1.37	NNLO(QCD)+NLO(EW)
$q\bar{q}' \to ZH$	POWHEG-BOX	PYTHIA 8	PDF4LHC15	0.76	NNLO(QCD)+NLO(EW)
$gg \to ZH$	POWHEG-BOX	PYTHIA 8	PDF4LHC15	0.12	NNLO(QCD)+NLO(EW)
$t\bar{t}H$	POWHEG-BOX	PYTHIA 8	PDF4LHC15	0.51	NNLO(QCD)+NLO(EW)
$b\bar{b}H$	POWHEG-BOX	PYTHIA 8	PDF4LHC15	0.49	NNLO(QCD)+NLO(EW)
tHq	MG5_AMC@NLO	PYTHIA 8	CT10	0.07	4FS(LO)
tHW	MG5_AMC@NLO	Herwig++	CT10	0.02	5FS(NLO)
$\gamma\gamma$	SHERPA	SHERPA	CT10		
$V\gamma\gamma$	SHERPA	SHERPA	CT10		
$t\bar{t}\gamma\gamma$	MG5_AMC@NLO	PYTHIA 8	PDF4LHC15		

Process	Measurement region	Stage-1 region
ggF + $gg \to Z(\to qq)H$	0-jet	0-jet
	1-jet, $p_T^H < 60\,GeV$	1-jet, $p_T^H < 60\,GeV$
	1-jet, $60 \le p_T^H < 120\,GeV$	1-jet, $60 \le p_T^H < 120\,GeV$
	1-jet, $120 \le p_T^H < 200\,GeV$	1-jet, $120 \le p_T^H < 200\,GeV$
	BSM-like* ($\ge$ 1-jet, $p_T^H > 200\,GeV$)	1-jet, $p_T^H > 200\,GeV$
		$\ge$ 2-jet, $p_T^H > 200\,GeV$
	$\ge$ 2 jet ($p_T^H < 200\,GeV$ or VBF-like)	$\ge$ 2-jet, $p_T^H < 60\,GeV$
		$\ge$ 2-jet, $60 \le p_T^H < 120\,GeV$
		$\ge$ 2-jet, $120 \le p_T^H < 200\,GeV$
		VBF-like, $p_T^{Hjj} < 25\,GeV$
		VBF-like, $p_T^{Hjj} \ge 25\,GeV$
$qq' \to Hqq'$ (VBF + VH hadronic)	$p_T^j < 200\,GeV$	$p_T^j < 200\,GeV$, VBF-like, $p_T^{Hjj} < 25\,GeV$
		$p_T^j < 200\,GeV$, VBF-like, $p_T^{Hjj} \ge 25\,GeV$
		$p_T^j < 200\,GeV$, VH-like
		$p_T^j < 200\,GeV$, Rest
	BSM-like* ($p_T^j > 200\,GeV$)	$p_T^j > 200\,GeV$
VH (leptonic decays)	VH leptonic	$q\bar{q} \to ZH$, $p_T^Z < 150$ GeV
		$q\bar{q} \to ZH$, 150 GeV $< p_T^Z <$ 250 GeV, 0-jet
		$q\bar{q} \to ZH$, 150 GeV $< p_T^Z <$ 250 GeV, $\ge$ 1-jet
		$q\bar{q} \to ZH$, $p_T^Z > 250$ GeV
		$q\bar{q} \to WH$, $p_T^W < 150$ GeV
		$q\bar{q} \to WH$, 150 GeV $< p_T^W <$ 250 GeV, 0-jet
		$q\bar{q} \to WH$, 150 GeV $< p_T^W <$ 250 GeV, $\ge$ 1-jet
		$q\bar{q} \to WH$, $p_T^W > 250$ GeV
		$gg \to ZH$, $p_T^Z < 150$ GeV
		$gg \to ZH$, $p_T^Z > 150$ GeV, 0-jet
		$gg \to ZH$, $p_T^Z > 150$ GeV, $\ge$ 1-jet
top-associated production	Top	$t\bar{t}H$
		tHW
		$tHqb$
$b\bar{b}H$	merged w/ ggF	$b\bar{b}H$

Category label	Selection
ttH lep BDT1	$N_{lep} \ge 1$, $N_{b-jet} \ge 1$, $BDT_{ttHlep} > 0.987$
ttH lep BDT2	$N_{lep} \ge 1$, $N_{b-jet} \ge 1$, $0.942 < BDT_{ttHlep} < 0.987$
ttH lep BDT3	$N_{lep} \ge 1$, $N_{b-jet} \ge 1$, $0.705 < BDT_{ttHlep} < 0.942$
ttH had BDT1	$N_{lep} = 0$, $N_{jets} \ge 3$, $N_{b-jet} \ge 1$, $BDT_{ttHhad} > 0.996$
ttH had BDT2	$N_{lep} = 0$, $N_{jets} \ge 3$, $N_{b-jet} \ge 1$, $0.991 < BDT_{ttHhad} < 0.996$
ttH had BDT3	$N_{lep} = 0$, $N_{jets} \ge 3$, $N_{b-jet} \ge 1$, $0.971 < BDT_{ttHhad} < 0.991$
ttH had BDT4	$N_{lep} = 0$, $N_{jets} \ge 3$, $N_{b-jet} \ge 1$, $0.911 < BDT_{ttHhad} < 0.971$
VH dilep	$N_{lep} \ge 2$, $70\,GeV \le m_{\ell\ell} \le 110\,GeV$
VH lep High	$N_{lep} = 1$, $\lvert m_{e\gamma} - 89\,GeV\rvert > 5\,GeV$, $p_T^{\ell+E_T^{miss}} > 150\,GeV$
VH lep Low	$N_{lep} = 1$, $\lvert m_{e\gamma} - 89\,GeV\rvert > 5\,GeV$, $p_T^{\ell+E_T^{miss}} < 150\,GeV$, E_T^{miss} significance > 1
VH MET High	$150\,GeV < E_T^{miss} < 250\,GeV$, E_T^{miss} significance > 9 or $E_T^{miss} > 250\,GeV$
VH MET Low	$80\,GeV < E_T^{miss} < 150\,GeV$, E_T^{miss} significance > 8
qqH BSM	$N_{jets} \ge 2$, $p_{T,j1} > 200\,GeV$
VH had BDT tight	$60\,GeV < m_{jj} < 120\,GeV$, $BDT_{VH} > 0.78$
VH had BDT loose	$60\,GeV < m_{jj} < 120\,GeV$, $0.35 < BDT_{VH} < 0.78$
VBF high-p_T^{Hjj} BDT tight	$\lvert\Delta\eta_{jj}\rvert > 2$, $\lvert\eta_{\gamma\gamma} - 0.5(\eta_{j1}+\eta_{j2})\rvert < 5$, $p_T^{Hjj} > 25\,GeV$, $BDT_{VBF}^{high} > 0.47$
VBF high-p_T^{Hjj} BDT loose	$\lvert\Delta\eta_{jj}\rvert > 2$, $\lvert\eta_{\gamma\gamma} - 0.5(\eta_{j1}+\eta_{j2})\rvert < 5$, $p_T^{Hjj} > 25\,GeV$, $-0.32 < BDT_{VBF}^{high} < 0.47$
VBF low-p_T^{Hjj} BDT tight	$\lvert\Delta\eta_{jj}\rvert > 2$, $\lvert\eta_{\gamma\gamma} - 0.5(\eta_{j1}+\eta_{j2})\rvert < 5$, $p_T^{Hjj} < 25\,GeV$, $BDT_{VBF}^{low} > 0.87$
VBF low-p_T^{Hjj} BDT loose	$\lvert\Delta\eta_{jj}\rvert > 2$, $\lvert\eta_{\gamma\gamma} - 0.5(\eta_{j1}+\eta_{j2})\rvert < 5$, $p_T^{Hjj} < 25\,GeV$, $0.26 < BDT_{VBF}^{low} < 0.87$
ggF 2J BSM	$N_{jets} \ge 2$, $p_T^{\gamma\gamma} \ge 200\,GeV$
ggF 2J High	$N_{jets} \ge 2$, $p_T^{\gamma\gamma} \in [120, 200]$ GeV
ggF 2J Med	$N_{jets} \ge 2$, $p_T^{\gamma\gamma} \in [60, 120]$ GeV
ggF 2J Low	$N_{jets} \ge 2$, $p_T^{\gamma\gamma} \in [0, 60]$ GeV
ggF 1J BSM	$N_{jets} = 1$, $p_T^{\gamma\gamma} \ge 200\,GeV$
ggF 1J High	$N_{jets} = 1$, $p_T^{\gamma\gamma} \in [120, 200]$ GeV
ggF 1J Med	$N_{jets} = 1$, $p_T^{\gamma\gamma} \in [60, 120]$ GeV
ggF 1J Low	$N_{jets} = 1$, $p_T^{\gamma\gamma} \in [0, 60]$ GeV
ggF 0J Fwd	$N_{jets} = 0$, one photon with $\lvert\eta\rvert > 0.95$
ggF 0J Cen	$N_{jets} = 0$, two photons with $\lvert\eta\rvert \le 0.95$

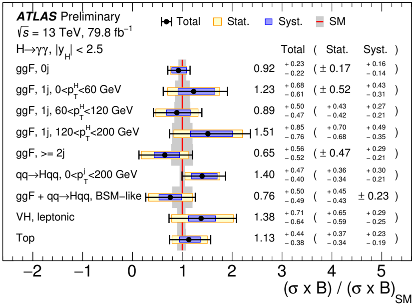

ATLAS Preliminary
√s = 13 TeV, 79.8 fb⁻¹
H→γγ, |y_H| < 2.5
Total
Stat.
Syst.
SM
Total (Stat. Syst.)
ggF, 0j 0.92 +0.23 −0.22 (± 0.17 +0.16 −0.14)
ggF, 1j, 0<p_T^H<60 GeV 1.23 +0.68 −0.61 (± 0.52 +0.43 −0.31)
ggF, 1j, 60<p_T^H<120 GeV 0.89 +0.50 −0.47 (+0.43 −0.42 +0.27 −0.21)
ggF, 1j, 120<p_T^H<200 GeV 1.51 +0.85 −0.76 (+0.70 −0.68 +0.49 −0.35)
ggF, >= 2j 0.65 +0.56 −0.52 (± 0.47 +0.29 −0.21)
qq→Hqq, 0<p_T^j<200 GeV 1.40 +0.47 −0.40 (+0.36 −0.34 +0.30 −0.21)
ggF + qq→Hqq, BSM−like 0.76 +0.50 −0.49 (+0.45 −0.43 ± 0.23)
VH, leptonic 1.38 +0.71 −0.64 (+0.65 −0.59 +0.29 −0.25)
Top 1.13 +0.44 −0.38 (+0.37 −0.34 +0.23 −0.19)
−2 −1 0 1 2 3 4 5
(σ x B) / (σ x B)_SM

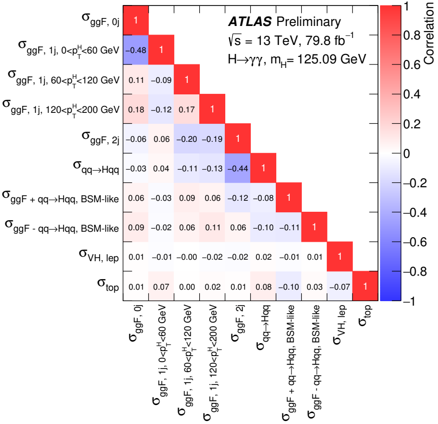

ATLAS Preliminary
√s = 13 TeV, 79.8 fb⁻¹
H→γγ, m_H= 125.09 GeV
Correlation
σ_ggF, 0j
σ_ggF, 1j, 0<p_T^H<60 GeV
σ_ggF, 1j, 60<p_T^H<120 GeV
σ_ggF, 1j, 120<p_T^H<200 GeV
σ_ggF, 2j
σ_qq→Hqq
σ_ggF + qq→Hqq, BSM-like
σ_ggF - qq→Hqq, BSM-like
σ_VH, lep
σ_top
1
−0.48 1
0.11 −0.09 1
0.18 −0.12 0.17 1
−0.06 0.06 −0.20 −0.19 1
−0.03 0.04 −0.11 −0.13 −0.44 1
0.06 −0.03 0.09 0.06 −0.12 −0.08 1
0.09 −0.02 0.06 0.11 0.06 −0.10 −0.11 1
0.01 −0.01 −0.00 −0.02 −0.02 0.02 −0.01 0.01 1
0.01 0.07 0.00 0.02 0.01 0.08 −0.10 0.03 −0.07 1
1 0.8 0.6 0.4 0.2 0 −0.2 −0.4 −0.6 −0.8 −1

Theory comparisons for differential distributions

The unfolded differential distributions are compared to state-of-the art theory predictions of gluon fusion production. Contributions from the other production modes are modeled using the XH simulated samples described in Section 9.3 and added to each gluon-fusion prediction before comparing to data. All data distributions are compared to:

- the default MC prediction (Powheg NNLOPS normalized with the N^{3}LO in QCD and NLO EW cross section) introduced in Section 9.3.

Additionally, the $p_T^{\gamma\gamma}$ distribution is compared to:

- NNLOjet+SCET [99], which provides predictions using a N^{3}LL resummation matched to an NNLO fixed-order calculation in the heavy top limit. Additional corrections are applied for the fiducial selections of the analysis and are obtained from the default MC sample (Powheg NNLOPS). The prediction is corrected to account for the efficiency of the particle-level photon isolation [7].

The $|y_{\gamma\gamma}|$ distribution is compared to:

- SCETlib+MCFM8, which provides predictions for $|y_{\gamma\gamma}|$ at NNLO+NNLL$'_\varphi$ accuracy, derived by applying a resummation of the virtual corrections to the gluon form factor [100, 101].[5] The underlying NNLO predictions are obtained using MCFM8 with zero-jettiness subtractions [102, 103]. The prediction is corrected for the particle-level photon isolation efficiency.

The $p_T^{j_1}$ distribution is compared to:

- The parton-level NNLOjet prediction of Refs. [104, 105], a fixed-order NNLO prediction in QCD for inclusive $H + 1$-jet production. The NNLOjet prediction is compared to data in the phase space with at least 1 jet.
- SCETlib(STWZ) [89, 101], which provides predictions for $p_T^{j_1}$ at NNLL$'$+NNLO$_0$ accuracy are derived applying a resummation in $p_T^{j_1}$.

Both the NNLOjet and SCETlib predictions for $p_T^{j_1}$ are corrected for the particle-level photon isolation efficiency.

[99] X. Chen et al., *Precise QCD Description of the Higgs Boson Transverse Momentum Spectrum*, (2018), arXiv: 1805.00736 [hep-ph].

[100] M. A. Ebert, J. K. L. Michel and F. J. Tackmann, *Resummation improved rapidity spectrum for gluon fusion Higgs production*, JHEP **05** (2017) 088, arXiv: 1702.00794 [hep-ph].

[101] M. A. Ebert et al., *SCETlib: A C++ Package for Numerical Calculations in QCD and Soft-Collinear Effective Theory*, DESY-17-099, URL: http://scetlib.desy.de.

[102] R. Boughezal et al., *Color singlet production at NNLO in MCFM*, Eur. Phys. J. C **77** (2017) 7, arXiv: 1605.08011 [hep-ph].

[103] J. Gaunt, M. Stahlhofen, F. J. Tackmann and J. R. Walsh, *N-jettiness Subtractions for NNLO QCD calculations*, JHEP **09** (2015) 058, arXiv: 1505.04794 [hep-ph].

[104] X. Chen, T. Gehrmann, E. W. N. Glover and M. Jaquier, *Precise QCD predictions for the production of Higgs + jet final states*, Phys. Lett. B **740** (2015) 147, arXiv: 1408.5325 [hep-ph].

[105] X. Chen, J. Cruz-Martinez, T. Gehrmann, E. W. N. Glover and M. Jaquier, *NNLO QCD corrections to Higgs boson production at large transverse momentum*, JHEP **10** (2016) 066, arXiv: 1607.08817 [hep-ph].

Details of Higgs signal theory predictions

The production of the SM Higgs boson via gluon-gluon fusion (ggF), via vector boson fusion (VBF), associated with a vector boson (VH, where V is a W or a Z boson) and with a top quark pair (ttH) is modelled with the POWHEG-BOX v2 Monte Carlo (MC) event generator [23–27]. For ggF, the PDF4LHC next-to-next-to-leading-order (NNLO) set of parton distribution functions (PDF) is used, while for all other production modes, the PDF4LHC next-to-leading-order (NLO) set is used [28]. The event generator is interfaced to EvtGen v1.2.0 [29] for simulation of the bottom and charm hadron decays. The ggF Higgs boson production uses the POWHEG method for merging the NLO Higgs + jet cross section with the parton shower and the MiNLO method [30] to simultaneously achieve NLO accuracy for inclusive Higgs boson production. In a second step a reweighting procedure (NNLOPS), exploiting the Higgs boson rapidity distribution, is applied using the HNNLO program [31, 32] to achieve NNLO accuracy in the strong coupling constant α_s.

The matrix elements of the VBF, $q\bar{q} \to VH$ and ttH production mechanisms are calculated up to NLO in QCD. For VH production, the MiNLO method is used to merge 0- and 1-jet events [27, 33]. The $gg \to ZH$ contribution is modelled at leading order (LO) in QCD.

The production of a Higgs boson in association with a bottom quark pair (bbH) is simulated at NLO with MadGraph5_aMC@NLO v2.3.3 [34], using the NNPDF23 PDF set [35], while the production in association with a single top quark (tH) is simulated at NLO with MadGraph5_aMC@NLO v2.3.3 (tHW) and with MadGraph5 v2.3.3 (tHq), using the CT10nlo PDF set [36].

For all production mechanisms, the PYTHIA 8 [37] generator, using the AZNLO set of tuned parameter [38], is used for the $H \to ZZ^* \to 4\ell$ decay as well as for the parton shower modelling. All signal samples are simulated for a Higgs boson mass $m_H = 125$ GeV.

For additional cross checks, the ggF sample was also generated with MadGraph5_aMC@NLO. This simulation is accurate at NLO QCD accuracy for zero, one and two additional partons merged with the FxFx merging scheme [39, 40].

The Higgs boson production cross sections and decay branching ratios, as well as their uncertainties, are taken from Refs. [35, 41–48]. The ggF production is calculated with next-to-next-to-next-to-leading order (N^{3}LO) accuracy in QCD and has NLO electroweak (EW) corrections applied [49–55]. For VBF production, full NLO QCD and EW calculations are used with approximate NNLO QCD corrections [56, 57]. The qq- and qg-initiated VH production is calculated at NNLO in QCD and NLO EW corrections are applied [58–60], while gg-initiated VH production is calculated at NLO in QCD. The ttH [61–64], bbH [65–67] and tH [68] processes are calculated to NLO accuracy in QCD. The branching ratio for the $H \to ZZ^* \to 4\ell$ decay with $m_H = 125$ GeV is predicted to be 0.0124% [45, 69] in the SM using PROPHECY4F [70, 71], which includes the complete NLO QCD and EW corrections, and the interference effects between identical final-state fermions. Due to the latter, the expected branching ratios of the $4e$ and 4μ final states are about 10% higher than the branching ratios to $2e2\mu$ and $2\mu 2e$ final states. Table 1

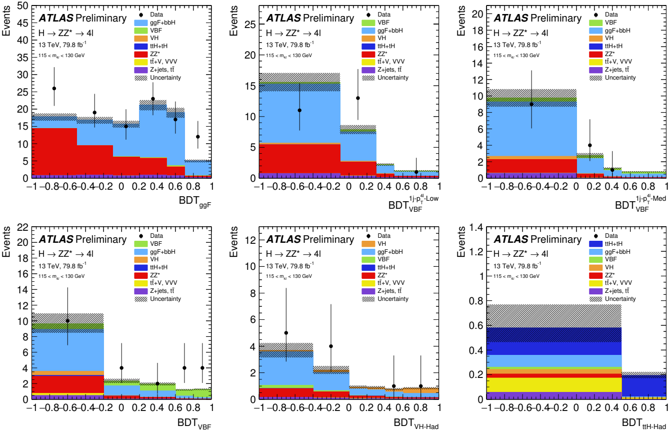

- Once split into event categories, individual BDTs are used to improve sensitivity to various production modes

Reconstructed event category	BDT discriminant	Input variables
$0j$-$p_T^{4\ell}$-Low	$\mathrm{BDT_{ggF}}$	$p_T^{4\ell}$, $\eta_{4\ell}$, D_{ZZ^*}
$1j$-$p_T^{4\ell}$-Low	$\mathrm{BDT}_{\mathrm{VBF}}^{1j\text{-}p_T^{4\ell}\text{-Low}}$	p_T^j, η_j, $\Delta R(j, 4\ell)$
$1j$-$p_T^{4\ell}$-Med	$\mathrm{BDT}_{\mathrm{VBF}}^{1j\text{-}p_T^{4\ell}\text{-Med}}$	p_T^j, η_j, $\Delta R(j, 4\ell)$
VBF-enriched-p_T^j-Low	$\mathrm{BDT_{VBF}}$	m_{jj}, $\Delta\eta_{jj}$, p_T^{j1}, p_T^{j2}, $\eta_{4\ell}^*$, $\Delta R_{jZ}^{\mathrm{min}}$, $p_T^{4\ell jj}$
VH-Had-enriched	$\mathrm{BDT}_{VH\text{-Had}}$	m_{jj}, $\Delta\eta_{jj}$, p_T^{j1}, p_T^{j2}, $\eta_{4\ell}^*$, $\Delta R_{jZ}^{\mathrm{min}}$, η_{j1}
ttH-Had-enriched	$\mathrm{BDT}_{ttH\text{-Had}}$	m_{jj}, $\Delta\eta_{jj}$, $\Delta R_{jZ}^{\mathrm{min}}$, $\Delta R(j, 4\ell)$, $\eta_{4\ell}^*$, E_T^{miss}, p_T^{jj}, N_{jets}, $N_{b-\mathrm{jets}}$, H_T, $\mathcal{M}_{sig}$

$H \rightarrow WW^*$ with ggH and VBF production I (arXiv:1808.09054)

Process	Matrix element (alternative)	PDF set	UEPS model (alternative model)	Prediction order for total cross-section
ggF H	Powheg-Box v2 NNLOPS [16,8,10] (MG5_aMC@NLO [44,45])	PDF4LHC15 NNLO [9]	Pythia 8 [14] (Herwig 7 [46])	N^3LO QCD + NLO EW [22,23,24,25,26]
VBF H	Powheg-Box v2 (MG5_aMC@NLO)	PDF4LHC15 NLO	Pythia 8 (Herwig 7)	NNLO QCD + NLO EW [22,27,28,29]
VH	Powheg-Box v2 [47]	PDF4LHC15 NLO	Pythia 8	NNLO QCD + NLO EW[48,49,50]
$qq \rightarrow WW$	Sherpa 2.2.2 [30,30,31] (Powheg-Box v2, MG5_aMC@NLO)	NNPDF3.0NNLO [32]	Sherpa 2.2.2 [33,34] (Herwig++ [46])	NLO [35]
$gg \rightarrow WW$	Sherpa 2.1.1 [35]	CT10 [51]	Sherpa 2.1	NLO [36]
$WZ/V\gamma^*/ZZ$	Sherpa 2.1	CT10	Sherpa 2.1	NLO [35]
$V\gamma$	Sherpa 2.2.2 (MG5_aMC@NLO)	NNPDF3.0NNLO	Sherpa 2.2.2 (CSS variation [33,52])	NLO [35]
$t\bar{t}$	Powheg-Box v2 [53] (Sherpa 2.2.1)	NNPDF3.0NLO	Pythia 8 (Herwig 7)	NNLO+NNLL [54]
Wt	Powheg-Box v1 [55] (MG5_aMC@NLO)	CT10 [51]	Pythia 6.428 [56] (Herwig++)	NLO [55]
Z/γ^*	Sherpa 2.2.1	NNPDF3.0NNLO	Sherpa 2.2.1	NNLO [57,58]

Category	$N_{\text{jet},(p_T>30\text{ GeV})} = 0$ ggF	$N_{\text{jet},(p_T>30\text{ GeV})} = 1$ ggF	$N_{\text{jet},(p_T>30\text{ GeV})} \geq 2$ VBF
Preselection	Two isolated, different-flavour leptons ($\ell = e, \mu$) with opposite charge		
	$p_T^{\text{lead}} > 22$ GeV , $p_T^{\text{sublead}} > 15$ GeV		
	$m_{\ell\ell} > 10$ GeV		
	$p_T^{\text{miss}} > 20$ GeV		
Background rejection	$N_{b\text{-jet},(p_T>20\text{ GeV})} = 0$		
	$\Delta\phi(\ell\ell, E_T^{\text{miss}}) > \pi/2$	$\max\left(m_T^{\ell}\right) > 50$ GeV	
	$p_T^{\ell\ell} > 30$ GeV	$m_{\tau\tau} < m_Z - 25$ GeV	
$H \rightarrow WW^* \rightarrow e\nu\mu\nu$	$m_{\ell\ell} < 55$ GeV, $\Delta\phi_{\ell\ell} < 1.8$		central jet veto, outside lepton veto
Discriminant variable	m_T		BDT
BDT input variables			m_{jj}, Δy_{jj}, $m_{\ell\ell}$, $\Delta\phi_{\ell\ell}$, m_T, $\sum_\ell C_\ell$, $\sum_{\ell,j} m_{\ell j}$, p_T^{tot}

Source	$\Delta\sigma_{\text{ggF}} \cdot \mathcal{B}_{H\rightarrow WW^*}$ [%]	$\Delta\sigma_{\text{VBF}} \cdot \mathcal{B}_{H\rightarrow WW^*}$ [%]
Data statistics	8	46
CR statistics	8	9
MC statistics	5	23
Theoretical uncertainties	8	21
ggF signal	5	15
VBF signal	<1	5
WW	5	12
Top-quark	4	4
Experimental uncertainties	9	8
b-tagging	5	6
Modelling of pile-up	5	2
Jet	3	4
Electron	3	<1
Misidentified leptons	5	9
Luminosity	2	3
TOTAL	17	59

Process	ME generator	ME PDF	PS and Hadronisation	UE model tune	Cross-section order
Signal, mass set to 125 GeV and $b\bar{b}$ branching fraction to 58%					
$qq \to WH$ $\to \ell\nu b\bar{b}$	Powheg-Box v2 [69] + GoSam [72] + MiNLO [73,74]	NNPDF3.0NLO$^{(\star)}$ [70]	Pythia 8.212 [61]	AZNLO [71]	NNLO(QCD)+ NLO(EW) [75–81]
$qq \to ZH$ $\to \nu\nu b\bar{b}/\ell\ell b\bar{b}$	Powheg-Box v2 + GoSam + MiNLO	NNPDF3.0NLO$^{(\star)}$	Pythia 8.212	AZNLO	NNLO(QCD)$^{(\dagger)}$+ NLO(EW)
$gg \to ZH$ $\to \nu\nu b\bar{b}/\ell\ell b\bar{b}$	Powheg-Box v2	NNPDF3.0NLO$^{(\star)}$	Pythia 8.212	AZNLO	NLO+ NLL [82–86]
Top quark, mass set to 172.5 GeV					
$t\bar{t}$	Powheg-Box v2 [87]	NNPDF3.0NLO	Pythia 8.230	A14 [88]	NNLO+NNLL [89]
s-channel	Powheg-Box v2 [90]	NNPDF3.0NLO	Pythia 8.230	A14	NLO [91]
t-channel	Powheg-Box v2 [90]	NNPDF3.0NLO	Pythia 8.230	A14	NLO [92]
Wt	Powheg-Box v2 [93]	NNPDF3.0NLO	Pythia 8.230	A14	Approximate NNLO [94]
Vector boson + jets					
$W \to \ell\nu$	Sherpa 2.2.1 [64, 95, 96]	NNPDF3.0NNLO	Sherpa 2.2.1 [97, 98]	Default	NNLO [99]
$Z/\gamma^* \to \ell\ell$	Sherpa 2.2.1	NNPDF3.0NNLO	Sherpa 2.2.1	Default	NNLO
$Z \to \nu\nu$	Sherpa 2.2.1	NNPDF3.0NNLO	Sherpa 2.2.1	Default	NNLO
Diboson					
$qq \to WW$	Sherpa 2.2.1	NNPDF3.0NNLO	Sherpa 2.2.1	Default	NLO
$qq \to WZ$	Sherpa 2.2.1	NNPDF3.0NNLO	Sherpa 2.2.1	Default	NLO
$qq \to ZZ$	Sherpa 2.2.1	NNPDF3.0NNLO	Sherpa 2.2.1	Default	NLO
$gg \to VV$	Sherpa 2.2.2	NNPDF3.0NNLO	Sherpa 2.2.2	Default	NLO

Selection	0-lepton	1-lepton: e sub-channel	1-lepton: μ sub-channel	2-lepton
Trigger	$E_{\mathrm{T}}^{\mathrm{miss}}$	Single lepton	$E_{\mathrm{T}}^{\mathrm{miss}}$	Single lepton
Leptons	0 *loose* leptons with $p_{\mathrm{T}} > 7$ GeV	1 *tight* electron $p_{\mathrm{T}} > 27$ GeV	1 *tight* muon $p_{\mathrm{T}} > 25$ GeV	2 *loose* leptons with $p_{\mathrm{T}} > 7$ GeV ≥ 1 lepton with $p_{\mathrm{T}} > 27$ GeV
met	> 150 GeV	> 30 GeV	–	–
$m_{\ell\ell}$	–	–		81 GeV $< m_{\ell\ell} <$ 101 GeV
Jets	Exactly 2 / Exactly 3 jets			Exactly 2 / ≥ 3 jets
Jet p_{T}	> 20 GeV for $\|\eta\| < 2.5$ > 30 GeV for $2.5 < \|\eta\| < 4.5$			
b-jets	Exactly 2 b-tagged jets			
Leading b-tagged jet p_{T}	> 45 GeV			
H_{T}	> 120 (2 jets), >150 GeV (3 jets)	–		–
$\min[\Delta\phi(\vec{E}_{\mathrm{T}}^{\mathrm{miss}}, \vec{\mathrm{jets}})]$	$> 20^{\circ}$ (2 jets), $> 30^{\circ}$ (3 jets)	–		–
$\Delta\phi(\vec{E}_{\mathrm{T}}^{\mathrm{miss}}, \vec{bb})$	$> 120^{\circ}$	–		–
$\Delta\phi(\vec{b}_1, \vec{b}_2)$	$< 140^{\circ}$	–		–
$\Delta\phi(\vec{E}_{\mathrm{T}}^{\mathrm{miss}}, \vec{p}_{\mathrm{T}}^{\mathrm{miss}})$	$< 90^{\circ}$	–		–
p_{T}^{V} regions	> 150 GeV			75 GeV $< p_{\mathrm{T}}^{V} <$ 150 GeV, > 150 GeV
Signal regions	–	$m_{bb} \geq 75$ GeV or $m_{\mathrm{top}} \leq 225$ GeV		Same-flavour leptons Opposite-sign charges ($\mu\mu$ sub-channel)
Control regions	–	$m_{bb} < 75$ GeV and $m_{\mathrm{top}} > 225$ GeV		Different-flavour leptons Opposite-sign charges

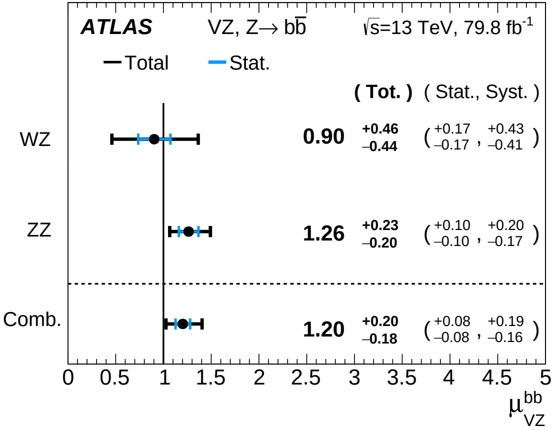

Results of the di-boson cross-check analysis

$H \to b\bar{b}$ with VH associated production I (arXiv:1808.08238)

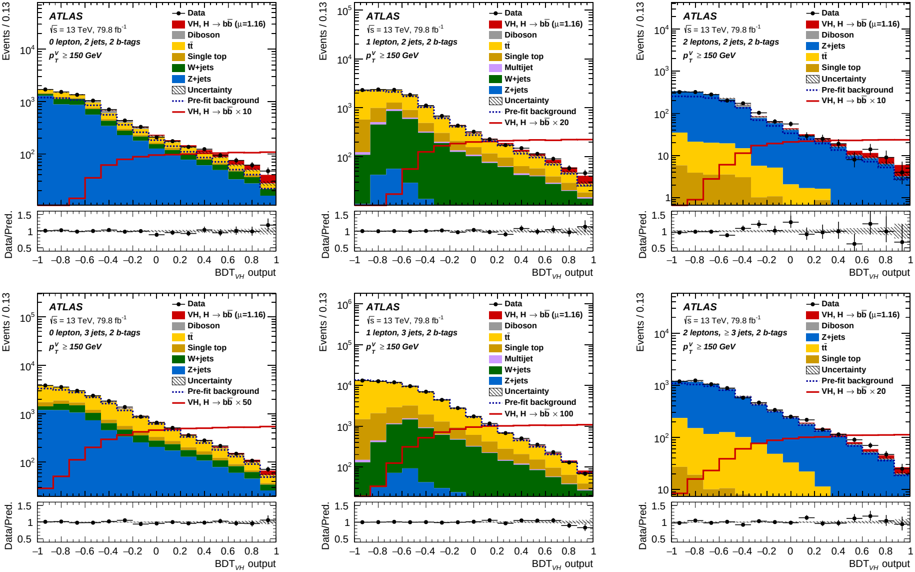

0 lepton: ↑ 2 jets ↓ 3 jets **1 lepton: ↑ 2 jets ↓ 3 jets** **2 lepton: ↑ 2 jets ↓ 3+ jets**

Combination of ATLAS Measurements (ATLAS-CONF-2018-031)

Production	Effective modifier	Resolved modifier
σ_{ggF}	κ_g^2	$1.04\,\kappa_t^2 + 0.002\,\kappa_b^2 - 0.04\,\kappa_t\kappa_b$
$\sigma_{V\mathrm{BF}}$	-	$0.73\,\kappa_W^2 + 0.27\,\kappa_Z^2$
$\sigma_{qq/qg\to ZH}$	-	κ_Z^2
$\sigma_{gg\to ZH}$	-	$2.46\,\kappa_Z^2 + 0.46\,\kappa_t^2 - 1.90\,\kappa_Z\kappa_t$
σ_{WH}	-	κ_W^2
$\sigma_{t\bar{t}H}$	-	κ_t^2
σ_{tHW}	-	$2.91\,\kappa_t^2 + 2.31\,\kappa_W^2 - 4.22\,\kappa_t\kappa_W$
σ_{tHq}	-	$2.63\,\kappa_t^2 + 3.58\,\kappa_W^2 - 5.21\,\kappa_t\kappa_W$
$\sigma_{b\bar{b}H}$	-	κ_b^2

Partial decay width	Effective modifier	Resolved modifier
$\Gamma_{\gamma\gamma}$	κ_γ^2	$1.59\,\kappa_W^2 + 0.07\,\kappa_t^2 - 0.67\,\kappa_W\kappa_t$
Γ_{ZZ}	-	κ_Z^2
Γ_{WW}	-	κ_W^2
$\Gamma_{\tau\tau}$	-	κ_τ^2
Γ_{bb}	-	κ_b^2
$\Gamma_{\mu\mu}$	-	κ_μ^2
Γ_{gg}	κ_g^2	$1.11\,\kappa_t^2 + 0.01\,\kappa_b^2 - 0.12\,\kappa_t\kappa_b$
$\Gamma_{Z\gamma}$	$\kappa_{(Z\gamma)}^2$	$1.12\,\kappa_W^2 - 0.12\,\kappa_W\kappa_t$

Total width	Efective modifier	Resolved modifier
Γ_H	κ_H^2	$(0.58\,\kappa_b^2 + 0.22\,\kappa_W^2 + 0.08\,\kappa_g^2 + 0.06\,\kappa_\tau^2 + 0.03\,\kappa_Z^2 + 0.03\,\kappa_c^2$ $+0.0023\,\kappa_\gamma^2 + 0.0015\,\kappa_{(Z\gamma)}^2 + 0.0004\,\kappa_s^2 + 0.00022\,\kappa_\mu^2)/(1 - \mathrm{B}_{\mathrm{BSM}})$

Combination of ATLAS Measurements (ATLAS-CONF-2018-031)

$H\to\gamma\gamma$	$H\to ZZ^*\to 4\ell$	$H\to WW^*$	$H\to\tau\tau$	$H\to b\bar{b}$
$t\bar{t}H$ leptonic (3 categories) $t\bar{t}H$ hadronic (4 categories)	$t\bar{t}H$ leptonic $t\bar{t}H$ hadronic	$t\bar{t}H$ multilepton 1 ℓ + 2 τ_{had} $t\bar{t}H$ multilepton 2 opposite-sign ℓ $t\bar{t}H$ multilepton 2 same-sign ℓ (categories for 0 or 1 τ_{had}) $t\bar{t}H$ multilepton 3 ℓ (categories for 0 or 1 τ_{had}) $t\bar{t}H$ multilepton 4 ℓ		$t\bar{t}H$ 1 ℓ, boosted $t\bar{t}H$ 1 ℓ, resolved (11 categories) $t\bar{t}H$ 2 ℓ (7 categories)
VH 2 ℓ VH 1 ℓ, $p_{\text{T}}^{\ell+E_{\text{T}}^{\text{miss}}} \geq 150$ GeV VH 1 ℓ, $p_{\text{T}}^{\ell+E_{\text{T}}^{\text{miss}}}$ ¡150 GeV VH $E_{\text{T}}^{\text{miss}}$, $E_{\text{T}}^{\text{miss}} \geq 150$ GeV VH $E_{\text{T}}^{\text{miss}}$, $E_{\text{T}}^{\text{miss}}$ ¡150 GeV VH+VBF $p_{\text{T}}^{j1} \geq 200$ GeV VH hadronic (2 categories)	VH leptonic 0-jet, $p_{\text{T}}^{4\ell} \geq 100$ GeV 2-jet, $m_{jj} < 120$ GeV			2 ℓ, $75 \leq p_{\text{T}}^{V} < 150$ GeV, $N_{\text{jets}} = 2$ 2 ℓ, $75 \leq p_{\text{T}}^{V} < 150$ GeV, $N_{\text{jets}} \geq 3$ 2 ℓ, $p_{\text{T}}^{V} \geq 150$ GeV, $N_{\text{jets}} = 2$ 2 ℓ, $p_{\text{T}}^{V} \geq 150$ GeV, $N_{\text{jets}} \geq 3$ 1 ℓ $p_{\text{T}}^{V} \geq 150$ GeV, $N_{\text{jets}} = 2$ 1 ℓ $p_{\text{T}}^{V} \geq 150$ GeV, $N_{\text{jets}} = 3$ 0 ℓ, $p_{\text{T}}^{V} \geq 150$ GeV, $N_{\text{jets}} = 2$ 0 ℓ, $p_{\text{T}}^{V} \geq 150$ GeV, $N_{\text{jets}} = 3$
VBF, $p_{\text{T}}^{\gamma\gamma jj} \geq 25$ GeV (2 categories) VBF, $p_{\text{T}}^{\gamma\gamma jj}$¡25 GeV (2 categories)	2-jet VBF, $p_{\text{T}}^{j1} \geq 200$ GeV 2-jet VBF, p_{T}^{j1}¡200 GeV	2-jet VBF	VBF $p_{\text{T}}^{\tau\tau} > 140$ GeV ($\tau_{\text{had}}\tau_{\text{had}}$ only) VBF high-m_{jj} VBF low-m_{jj}	
2-jet, $p_{\text{T}}^{\gamma\gamma} \geq 200$ GeV 2-jet, 120 GeV $\leq p_{\text{T}}^{\gamma\gamma}$¡200 GeV 2-jet, 60 GeV $\leq p_{\text{T}}^{\gamma\gamma}$¡120 GeV 2-jet, $p_{\text{T}}^{\gamma\gamma} < 60$ GeV 1-jet, $p_{\text{T}}^{\gamma\gamma} \geq 200$ GeV 1-jet, 120 GeV $\leq p_{\text{T}}^{\gamma\gamma}$¡200 GeV 1-jet, 60 GeV $\leq p_{\text{T}}^{\gamma\gamma}$¡120 GeV 1-jet, $p_{\text{T}}^{\gamma\gamma}$ ¡ 60 GeV 0-jet (2 categories)	1-jet, $p_{\text{T}}^{4\ell} \geq 120$ GeV 1-jet, 60 GeV$\leq p_{\text{T}}^{4\ell}$¡120 GeV 1-jet, $p_{\text{T}}^{4\ell} < 60$ GeV 0-jet, $p_{\text{T}}^{4\ell} < 100$ GeV	1-jet, $m_{\ell\ell} < 30$ GeV, $p_{\text{T}}^{\ell_2} < 20$ GeV 1-jet, $m_{\ell\ell} < 30$ GeV, $p_{\text{T}}^{\ell_2} \geq 20$ GeV 1-jet, $m_{\ell\ell} \geq 30$ GeV, $p_{\text{T}}^{\ell_2} < 20$ GeV 1-jet, $m_{\ell\ell} \geq 30$ GeV, $p_{\text{T}}^{\ell_2} \geq 20$ GeV 0-jet, $m_{\ell\ell} < 30$ GeV, $p_{\text{T}}^{\ell_2} < 20$ GeV 0-jet, $m_{\ell\ell} < 30$ GeV, $p_{\text{T}}^{\ell_2} \geq 20$ GeV 0-jet, $m_{\ell\ell} \geq 30$ GeV, $p_{\text{T}}^{\ell_2} < 20$ GeV 0-jet, $m_{\ell\ell} \geq 30$ GeV, $p_{\text{T}}^{\ell_2} \geq 20$ GeV	Boosted, $p_{\text{T}}^{\tau\tau} > 140$ GeV Boosted, $p_{\text{T}}^{\tau\tau} \leq 140$ GeV	

Uncertainty source	$\frac{\Delta\sigma_{\text{ggF}}}{\sigma_{\text{ggF}}}$ [%]	$\frac{\Delta\sigma_{VBF}}{\sigma_{VBF}}$ [%]	$\frac{\Delta\sigma_{WH}}{\sigma_{WH}}$ [%]	$\frac{\Delta\sigma_{ZH}}{\sigma_{ZH}}$ [%]	$\frac{\Delta\sigma_{t\bar{t}H+tH}}{\sigma_{t\bar{t}H+tH}}$ [%]
Total uncertainty	8.8	18	32	55	21
Statistical uncertainties	6.3	15	23	44	14
Systematic unc. (excl. MC stat.)	5.9	9.1	20	27	15
Theory uncertainties	3.3	6.2	16	21	12
Signal	2.1	5.5	11	8.6	5.9
Background	2.6	2.9	11	19	10
Experimental uncertainties	5.0	7.0	9.6	20	9.3
Luminosity	2.2	1.7	1.3	1.9	2.7
Fake leptons	1.6	1.7	0.5	0.8	5.5
Background modelling	2.0	1.4	6.0	8.1	0.9
Flavour tagging	0.8	1.4	4.8	14	1.6
Jets, $E_{\text{T}}^{\text{miss}}$	1.1	5.9	4.9	10	4.6
Electrons, photons	2.5	1.6	2.6	3.5	3.7
Muons	0.4	0.2	0.3	1.0	0.3
τ-lepton	0.2	1.4	0.6	0.7	2.4
Other	2.3	1.2	0.6	1.6	0.4
MC statistical uncertainties	1.5	5.1	9.6	19	4.4

Combination of ATLAS Measurements (ATLAS-CONF-2018-031)

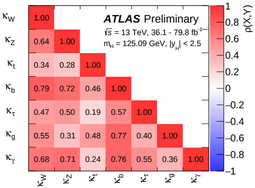

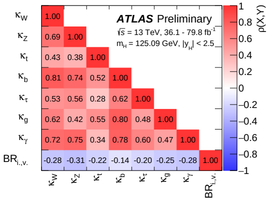

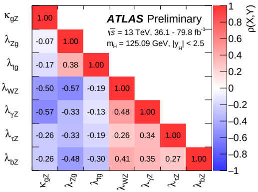

Left: $\mathcal{B}_{BSM} = 0$ fixed Centre: $\mathcal{B}_{BSM}$ free Right: κ ratios

5.5.1 Two Higgs doublet model

In 2HDMs, the SM Higgs sector is extended by introducing an additional complex isodoublet scalar field with weak hypercharge one. Four types of 2HDMs satisfy the Paschos-Glashow-Weinberg condition [83, 84], which prevents the appearance of tree-level flavor-changing neutral currents:

- Type I: one Higgs doublet couples to vector bosons, while the other one couples to fermions. The first doublet is 'fermiophobic' in the limit where the two Higgs doublets do not mix.
- Type II: one Higgs doublet couples to up-type quarks and the other one to down-type quarks and charged leptons.
- Lepton-specific: the Higgs bosons have the same couplings to quarks as in the Type I model and to charged leptons as in Type II.
- Flipped: the Higgs bosons have the same couplings to quarks as in the Type II model and to charged leptons as in Type I.

The observed Higgs boson is identified with the light CP-even neutral scalar h predicted by 2HDMs, and its accessible production and decay modes are assumed to be the same as those of the SM Higgs boson. Its couplings to vector bosons, up-type quarks, down-type quarks and leptons relative to the corresponding SM predictions are expressed as functions of the mixing angle of h with the heavy CP-even neutral scalar, α, and the ratio of the vacuum expectation values of the Higgs doublets, $\tan\beta$.

Figure 13 shows the regions of the $(\cos(\beta-\alpha), \tan\beta)$ plane that are excluded at a confidence level of 95 % or higher, for each of the four types of 2HDMs. The expected exclusion limits in the SM hypothesis are also overlaid. The data are consistent with the alignment limit [76] at $\cos(\beta-\alpha) = 0$, in which the couplings of h match those of the SM Higgs boson, within one standard deviation or better in each of the tested models. The allowed regions also include narrow, curved 'petal' regions at positive $\cos(\beta-\alpha)$ and moderate $\tan\beta$ in the Type II, Lepton-specific, and Flipped models. These correspond to regions with $\cos(\beta+\alpha) \approx 0$, for which some fermion couplings have the same magnitude as in the SM, but the opposite sign.

5.5.2 Simplified Minimal Supersymmetric Standard Model

The Minimal Supersymmetric Standard Model (MSSM) [85–87] is a realization of a Type II 2HDM. As a benchmark, a simplified MSSM model in which the Higgs boson is identified with the light CP-even scalar h, termed hMSSM [88–90], is studied. The assumptions made by this model are discussed in Ref. [23]. The production and decay modes accessible to h are assumed to be the same as those of the SM Higgs boson.

The Higgs boson couplings to vector bosons, up-type fermions and down-type fermions relative to the corresponding SM predictions are expressed as functions of the ratio of the vacuum expectation values of the Higgs doublets, $\tan\beta$, and the masses of the CP-odd scalar (m_A), the Z boson, and of h.

Figure 14 shows the regions of the hMSSM parameter space that are indirectly excluded by the measurement of the Higgs boson production and decay rates. The data are consistent with the SM decoupling limit at large m_A, where h couplings tend to those of the SM Higgs boson. The observed (expected) lower limit at 95 % CL on the CP-odd Higgs boson mass is at least $m_A > 520$ GeV ($m_A > 400$ GeV) for $1 \leq \tan\beta \leq 25$, increasing to $m_A > 580$ GeV ($m_A > 450$ GeV) at $\tan\beta = 1$.

The production of Higgs boson in association with a charm quark is directly sensitive to the charm quark Yukawa coupling

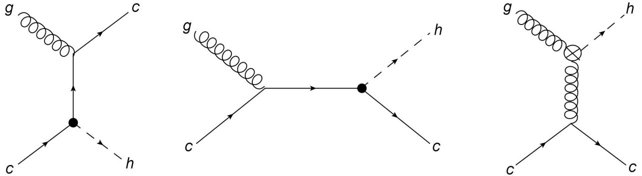

↑ **Examples of "direct" (left and centre) and "indirect" (right) $cg \to Hc$ diagrams (from arXiv:1507.02916)**

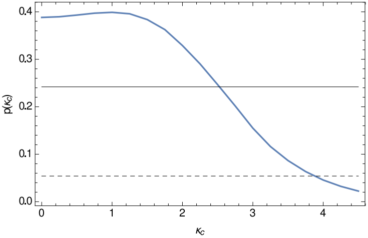

↑ **Expected p-value as a function of $\kappa_c = y_c/y_c^{SM}$ (from arXiv:1507.02916)**

- While "indirect" diagram (right) is expected to dominate, the cross-section is still very sensitive to the $Hc\bar{c}$ coupling!
- No experimental measurements yet, though the sensitivity at the HL-LHC has been surveyed in the literature (arXiv:1507.02916)
- Assuming a data sample of $3\,\text{ab}^{-1}$ at $\sqrt{s} = 14$ TeV, $\mathcal{O}(1)$ constraints on y_c/y_c^{SM} are expected to be obtained...

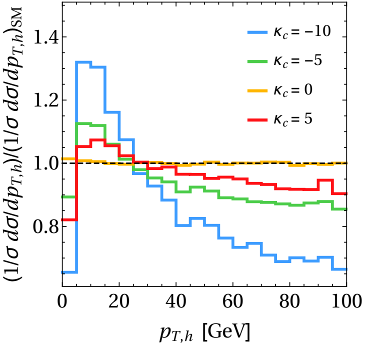

Effect of modified y_c on p_T^H from $cg \to Hc$ diagrams

(Phys. Rev. Lett. 118, 121801 (2017), arXiv:1606.09253)

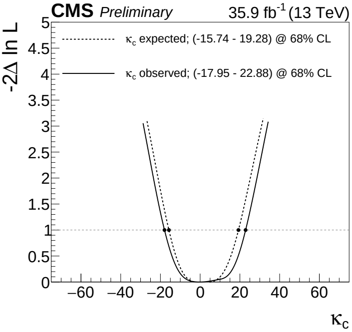

Bound on y_c/y_c^{SM} from Run 2 CMS data

(CMS-PAS-HIG-17-028)

- In the case of a modified Higgs coupling to heavy quarks $Q = c, b$, the shape of the inclusive p_T^H spectrum would change due to the modified $gQ \to HQ$ contribution
- Recently, CMS used their measured p_T^H distribution from $H \to \gamma\gamma$ and $H \to 4\ell$ accounting for dependence on y_c (and y_b)
- Considering only shape variation (no assumption on Γ_H, less model dependent) and profiling y_b/y_b^{SM}, obtain constrain of $-18 < y_c/y_c^{SM} < 23$ at 68% CL

- **Lifetime:** Long enough to lead to a measureable decay length (around 5mm for a 50 GeV boost)
- **Mass:** Weakly decaying *b*-hadrons have masses around 5 GeV, leading to high decay product multiplicities (average of 5 charged particles per decay)
- **Fragmentation:** Much harder than jets initiated by other species (*b*-hadrons carry around 75% of jet energy, on average)

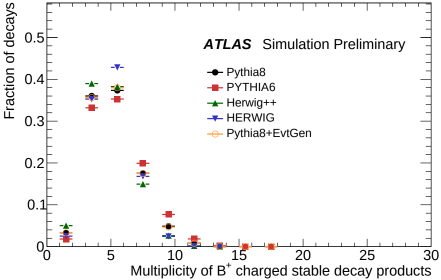

Left: Mean charged multiplicity in B^+ mesons decays

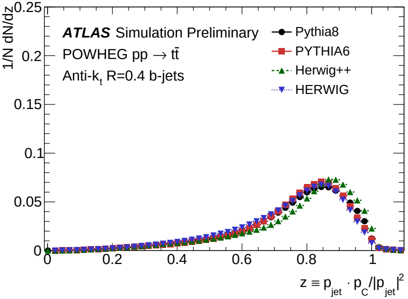

Right: *b*-quark fragmentation function

- **Lifetime:** Shorter than the *b*-hadrons by around a factor of 2-3, still enough for measureable decay length (around 1-3mm for a 50 GeV boost)
- **Mass:** Weakly decaying *c*-hadrons have masses around 2 GeV, around 2–3× lower than *b*-hadrons (mean of ≈ 2 charged particles per decay)
- **Fragmentation:** Softer than *b*-jets, but still harder than jets initiated by light species (*c*-hadrons carry around 55% of jet energy, on average)

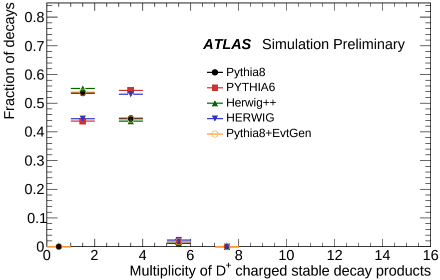

Left: Mean charged multiplicity in D^+ mesons decays

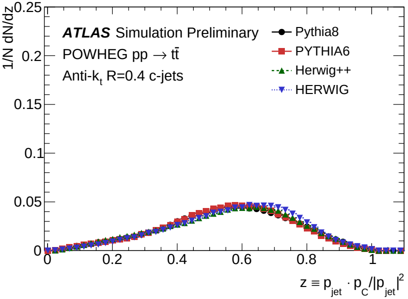

Right: *c*-quark fragmentation function

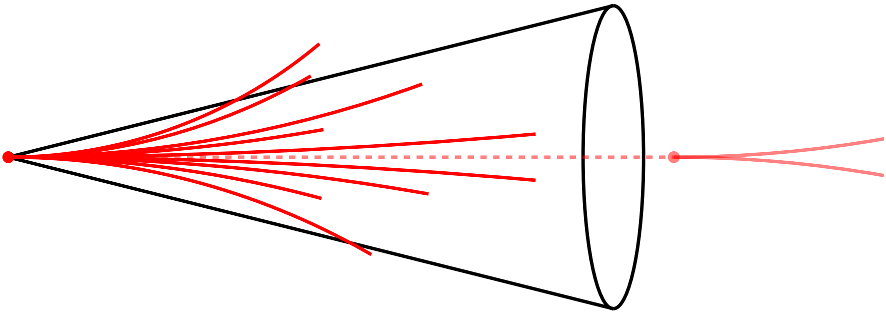

Typical Experimental Signature

- Light-quarks hadronise into many light hadrons which share the jet energy
- Tracks from this vertex often have impact parameters consistent with zero
- Long-lived light hadrons (e.g. K_S^0, Λ^0) can be produced, though they are more likely to decay very far (many cm) from the primary *pp* vertex

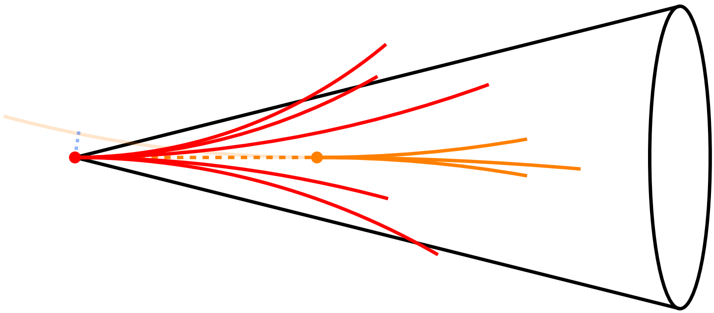

Typical Experimental Signature

- ***c*-quark fragments into a *c*-hadron which carries around half of the jet energy**
- ***c*-hadron decay vertex often displaced from the primary *pp* vertex by a few mm**
- **Tracks from this vertex can often have large impact parameters**

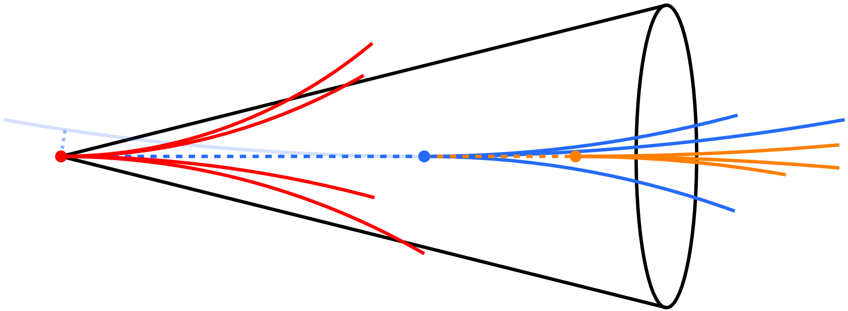

Typical Experimental Signature

- *b*-quark fragments into a *b*-hadron which carries most of the jet energy
- Most *b*-hadrons ($\approx 90\%$) decay into *c*-hadrons
- *b*-hadron decay vertex often displaced from the primary *pp* vertex by a few mm
- Subsequent *c*-hadron decay vertex often displaced by a further few mm
- Tracks from both of these vertices often have large impact parameters

Charm tagging is not new, many experiments at high energy ($\sqrt{s} \gg m_{B\bar{B}}$) colliders (e.g. Sp$\bar{\text{p}}$S, Tevatron, SLD, LEP, HERA) have built "charm taggers" which tend to fall within the following classes:

"Exclusive" charm jet tagging

- Focus on the full reconstruction of exclusive c-hadron decay chains (e.g. $D^{\star\pm} \to D^0(K^-\pi^+)\pi^\pm$) or leptons from semi-leptonic c-hadron decays
- ✓ Can often provide a very pure sample of jets containing c-hadrons
- ✗ The efficiency is typically low $\mathcal{O}(1\%)$, limited by the c-hadron branching fractions of interest

"Inclusive" charm jet tagging

- An alternative approach is to to exploit more "inclusive" observables, such as track impact parameters or secondary vertices
- ✓ The efficiency of this approach is typically very high $\mathcal{O}(10\%)$)
- ✗ The c-jet purity is often lower than these "traditional" approaches
- More suited for use with machine learning (ML) techniques

ATLAS have developed an "inclusive" c-tagging algorithm based on several "low level" taggers combined into a "high level" tagger using ML techniques

The signed IPs of tracks associated to jets are powerful jet flavour distriminants:

- Exploit "sign" of impact parameter: positive if track point of closest approach to PV is downstream of plane defined by the PV and jet axis
- Tracks from *b*-hadrons tend to have highly significant (IP/σ_{IP}) positive IPs, while most tracks from the PV have a narrow, symmetric distribution
- ✓ Very inclusive and highly efficient
- ✗ Relies upon accurate measurement of jet axis, sensitive to "mis-tag" high IP tracks from V^0 decays or material interactions, IP/σ_{IP} difficult to model in detector simulation

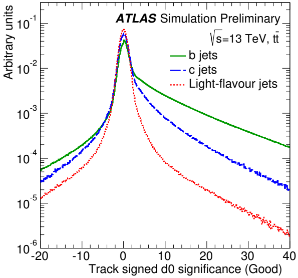

Left: Transverse IP significance distribution

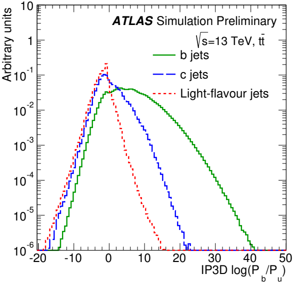

Right: likelihood ratio discriminant based on 3D IPs of tracks

ATLAS Low Level Taggers: 2 - Secondary Vertices (SV)

Exploit expectation of a secondary vertex from either *b* or *c*-hadron decays:

- Attempt to reconstruct a secondary vertex from high IP tracks associated with jet
- Use invariant mass of tracks at SV to discriminate *b* or *c*-hadron decay vertices from V^0 decays or material interations
- Exploit hard c/b-jet fragmentation, SV should carry a large fraction of jet energy
- ✓ SV found in up to ≈ 80% of *b*-jets but only a few % of light flavour jets
- ✗ Degraded light jet rejection as jet p_T increases, careful considerations to mitigate "tagging" of material interactions required

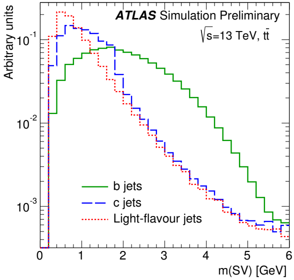

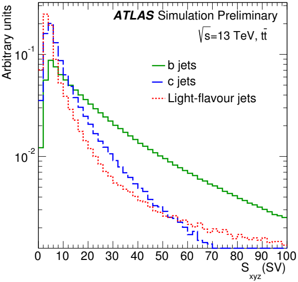

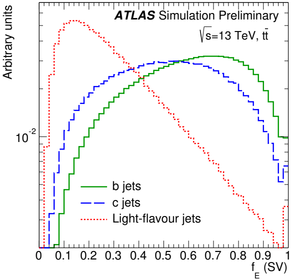

Left: Inv. mass of tracks at SV **Centre: 3D SV decay length significance** **Right: Energy fraction of SV tracks**

Exploit common occurance of cascade decay chain; *b*-hadron → *c*-hadron:

- Use Kalman filter to search for common axis on which three vertices lie: primary (pp) → secondary (b-hadron) → tertiary (c-hadron)
- Can then look for "1 track vertices" with decay chain axis
- ✓ Addition of 1 track vertices improves efficiency, constraint to decay chain axis improves separation power of SV based discriminants
- ✗ Degraded performance for c/b-hadron vertices as jet p_T increases, high fake rate for 1 track vertices (increases light jet "mis-tag" rate)

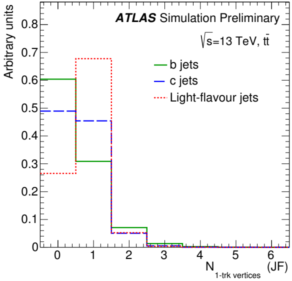

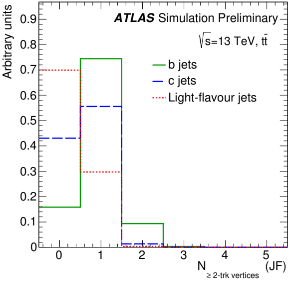

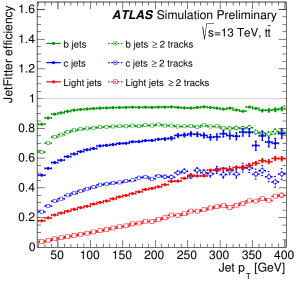

Left: Multiplicity of 1 track vertices **Centre: Multiplicity of 2+ track vertices** **Right: Reco. efficiency vs. jet p_T**

- In $\sqrt{s} = 13$ TeV pp collisions, Higgs boson production in association with a Z boson represents around 1.6% of the inclusive production rate
- The cross-section is dominated by the $q\bar{q} \to ZH$ process, with total cross-section $\sigma_{q\bar{q}} \approx 0.76\,\text{pb}$
- Smaller contributions from $gg \to ZH$, with total cross-section $\sigma_{gg} \approx 0.12\,\text{pb}$, though it exhibits a harder p_T^H spectrum below ≈ 150 GeV

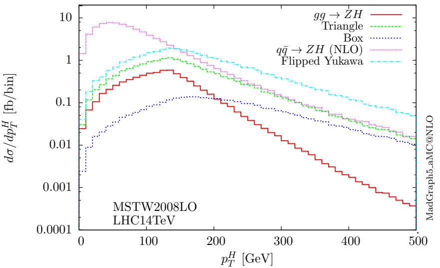

↑ **p_T^H distribution for $q\bar{q}$ and gg initiated ZH production (from arXiv:1503.01656)**

Representative Feynman diagrams for $q\bar{q}/gg \to ZH$ processes →

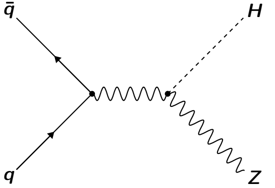

$q\bar{q} \to ZH$ diagram

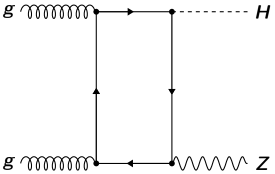

$gg \to ZH$ "box" diagram

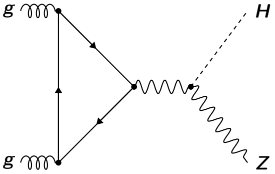

$gg \to ZH$ "triangle" diagram

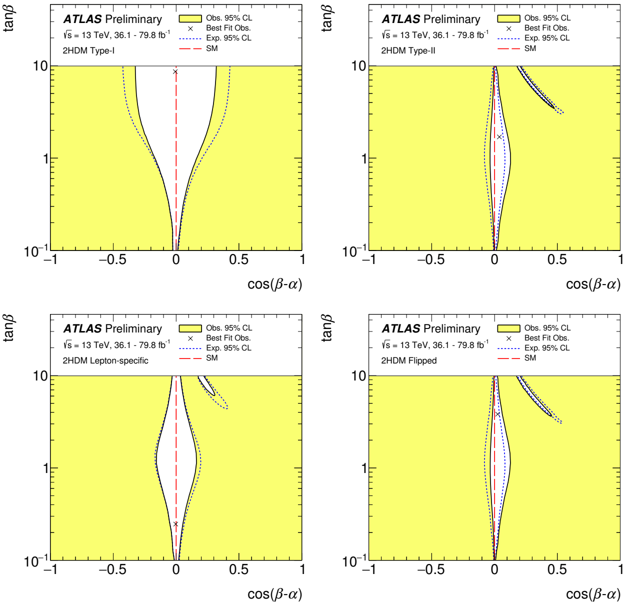

Constraints on 2HDM models

- Observed Higgs boson is identified with the light CP-even neutral scalar *h*
- 95% CL limits set in $\tan\beta - \cos\beta - \alpha$ plane
- Only region very close to "alignment limit" left
- Other small "petal" regions correspond to $\cos(\alpha+\beta) \approx 0$, where fermion couplings are close to SM magnitude but with opposite sign

$ZH, H \to c\bar{c}$ Background Composition

Sample	Yield, 50 $GeV < m_{c\bar{c}} <$ 200 GeV			
	1 c-tag		2 c-tags	
	$75 \leq p_{\mathrm{T}}^{Z} < 150\,GeV$	$p_{\mathrm{T}}^{Z} \geq 150\,GeV$	$75 \leq p_{\mathrm{T}}^{Z} < 150\,GeV$	$p_{\mathrm{T}}^{Z} \geq 150\,GeV$
$Z +$ jets	69400 ± 500	15650 ± 180	5320 ± 100	1280 ± 40
ZW	750 ± 130	290 ± 50	53 ± 13	20 ± 5
ZZ	490 ± 70	180 ± 28	55 ± 18	26 ± 8
$t\bar{t}$	2020 ± 280	130 ± 50	240 ± 40	13 ± 6
$ZH(b\bar{b})$	32 ± 2	19.5 ± 1.5	4.1 ± 0.4	2.7 ± 0.2
$ZH(c\bar{c})$ (SM)	-143 $\pm$ 170 (2.4)	-84 $\pm$ 100 (1.4)	-30 $\pm$ 40 (0.7)	-20 $\pm$ 29 (0.5)
Total	72500 ± 320	16180 ± 140	5650 ± 80	1320 ± 40
Data	72504	16181	5648	1320

Top: κ_c vs. κ_b **Bottom: κ_c, profiling κ_b**

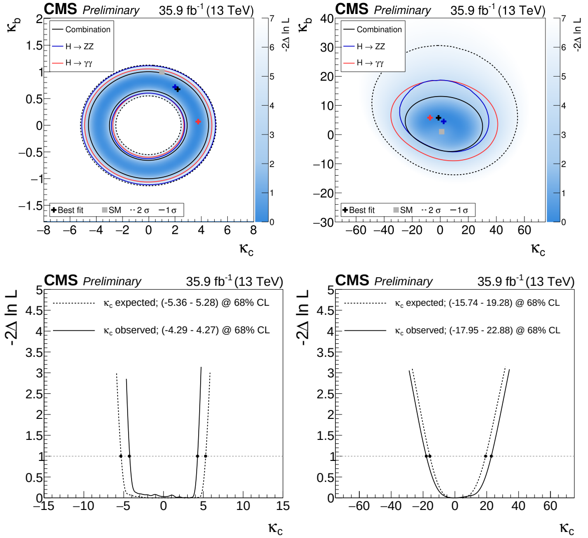

Left: Normalisation + shape information **Right: Only shape information**

ATLAS $H \to J/\psi\,\gamma$ Search - Constraint on κ_c/κ_γ

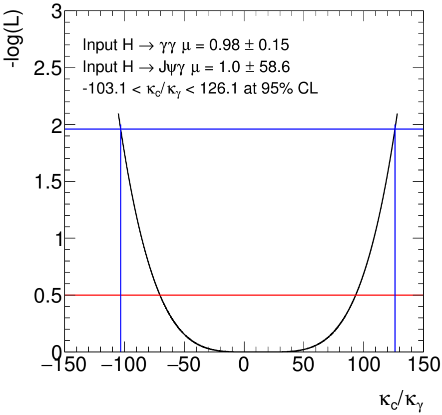

- Consider the ratio of signal strength measurements for $H \to J/\psi\,\gamma$ w.r.t. $H \to \gamma\gamma$
- Dependence on Γ_H and $\sigma(pp \to H)$ (approximately) cancels in this ratio, sensitive to κ_c/κ_γ
- Figure above based on ATLAS Run 2 $H \to J/\psi\,\gamma$ search and latest $H \to \gamma\gamma$ measurement (arXiv:1802.04146)

⚠ **This is NOT an ATLAS result, but my estimate based on public information alone**